Master of Science Thesis Aerospace Engineering

WIND FORECAST DRIVEN TRAJECTORY UNCERTAINTY IN IDLE DESCENTS

Y.Q.F. Karelsz

TU Delft

knowledge & development centre
Mainport Schiphol

Wind Forecast Driven Trajectory Uncertainty in Idle Descents

Thesis Report

by

Y.Q.F. Karelsz

to obtain the degree of Master of Science at the Delft University of Technology
to be defended publicly on July 1st, 2026 at 14:30

Student Number:	5087996
Project Duration:	September 2025 – June 2026
Place:	Faculty of Aerospace Engineering, Delft

Thesis Comittee

Chair:	Ir. P.C. Roling
Supervisor TU Delft:	Dr.ir. J. Ellerbroek
Supervisor KDC:	F. Dijkstra
External Examiner:	Dr. F. Orefice

Cover: Pinterest-KLM Boeing 737 (Hendrik van Beuningen)[5]

TU Delft

Preface

"Do or do not, there is no try."
– A childhood source of inspiration

This thesis marks the end of my academic journey of over two decades, from kindergarten all the way to a degree in Aerospace Engineering. Looking back, it has been a wonderful, interesting, and at times challenging experience.

I would like to thank my supervisors for their guidance throughout this project. I am grateful to Ferdinand Dijkstra for his enthusiasm and for motivating me to keep going, and to Joost Ellerbroek for the fresh perspectives he provided whenever I got lost in my own work.

Furthermore, I would like to extend my gratitude to my fellow iLabs students, who brightened up the long working days at LVNL. Of course, I would also like to thank my parents for their unconditional support throughout the years, and for giving me the freedom to chase my dreams and goals.

This project has challenged me beyond what I thought I was capable of. In the process, however, it has shown me what determination, curiosity, and perseverance can lead to. With that, I can confidently take the next step in my career.

Yoari Karelsz
June 2026, Delft

Contents

Nomenclature

Abbreviations

Abbreviation	Definition
ACC	Area Control Centre
ADS-C	Automatic Dependent Surveillance–Contract
AOC	Airline Operation Control
APP	Approach Control
ATC	Air Traffic Control
ATM	Air Traffic Management
BADA	Base of Aircraft Data
CAS	Calibrated Airspeed
CDA	Continuous Descent Approach
CDO	Continuous Descent Operation
CPDLC	Controller–Pilot Data Link Communications
CTA	Control Area
CTR	Control Zone
EHAM	ICAO airport code for Amsterdam Airport Schiphol
EPP	Extended Projected Profile
ESF	Energy Share Factor
ETA	Estimated Time of Arrival
FANS 1/A	Future Air Navigation System
FDR	Flight Data Recorder
FIR	Flight Information Region
FMS	Flight Management System
FPA	Flight Path Angle
GRIB	GRIdded Binary
GND	Ground Control
IAF	Initial Approach Fix
ICAO	International Civil Aviation Organization
KCAS	Knots Calibrated Airspeed
KDC	Knowledge Development Centre
KNMI	Royal Netherlands Meteorological Institute
LNAV	Lateral Navigation
LVNL	Air Traffic Control the Netherlands
MUAC	Maastricht Upper Area Control
OPD	Optimized Profile Descent
OTA	Oceanic Tailored Arrivals
RTA	Required Time of Arrival
STAR	Standard Terminal Arrival Route
TMA	Terminal Maneuvering Area
TOD	Top of Descent
TP	Trajectory Predictor
TWR	Tower Control
UTA	Upper Control Area
VNAV	Vertical Navigation
VPATH	Vertical Path mode (VNAV)
VSPEED	Speed Mode (VNAV)
WP	Work Package

Symbols

Symbol	Definition	Unit
Latin symbols		
D	Aerodynamic drag	[N]
E	Expected value, i.e. statistical mean	[–]
g	Surface gravity	[m/s^2]
h	Altitude	[m]
k	Gain	[–]
L	Aerodynamic lift	[N]
m	Aircraft mass	[kg]
t	Time	[s]
T	Thrust	[N]
ΔT	Time deviation, actual minus predicted	[s]
u, v	Vector components	[–]
V	Velocity magnitude	[m/s]
V_{CAS}	Calibrated airspeed	[m/s]
V_{g}	Ground speed	[m/s]
V_{T}	True airspeed	[m/s]
V_{V}	Vertical speed	[m/s]
V_{wind}	Wind component along the flight path	[m/s]
ΔV	Speed deviation, actual minus target	[m/s]
x, y, h	Inertial position components	[m]
$\hat{\mathbf{w}}_{\text{AC}}$	Actual wind vector	[m/s]
$\hat{\mathbf{w}}_{\text{FCST}}$	Forecast wind vector	[m/s]
Greek symbols		
α_T	Thrust angle	[deg]
γ	Aerodynamic flight-path angle	[deg]
γ_g	Geometric flight-path angle relative to the ground	[deg]
γ_{path}	Aerodynamic flight-path angle of the reference path	[deg]
ρ	Air density	[kg/m^3]
ρ_s	Spearman rank correlation coefficient	[-]
χ_{dr}	Drift angle	[deg]
ϕ	Roll angle	[deg]
ψ	Heading angle	[deg]

Subscripts

Subscript	Definition
AC	Actual condition
c	Commanded parameter
f	Forecast wind
FCST	Forecast
g	Ground-referenced quantity
o	True wind
path	Reference path quantity
ref	Reference trajectory
wx	Wind component in the x direction
wy	Wind component in the y direction

General Introduction

Aviation faces the challenge of accommodating growing traffic demand while reducing its environmental impact. At major hub airports such as Amsterdam Airport Schiphol, this challenge is particularly complex due to dense arrival streams, limited runway availability, and strict noise and emission constraints. Improving arrival operations therefore requires procedures that reduce fuel consumption and noise, while preserving the predictability and safety required for high-capacity air traffic management.

Idle descent operations provide an important opportunity in this regard. By allowing aircraft to descend continuously at or near idle thrust, fuel burn, noise, and unnecessary level segments can be reduced. However, this efficiency comes at the cost of reduced trajectory authority. During an idle descent, the aircraft has limited means to correct deviations without deploying thrust or spoilers, making the trajectory more sensitive to uncertainties in wind, aircraft performance, and flight management system behaviour.

This thesis focuses on the influence of descent wind forecast uncertainty on VNAV-PATH idle descents. Wind errors affect the aircraft both directly, by changing the groundspeed, and indirectly, by introducing energy-management errors that may appear as speed or path deviations. In dense arrival traffic, such deviations can reduce spacing predictability and may increase the likelihood of conflicts and loss-of-separations.

To investigate these effects, a simulation framework is developed that combines aircraft performance modeling, meteorological forecast data, reconstructed descent wind profiles, and representative Schiphol arrival scenarios. The framework is used to quantify how forecast horizon and wind profile reconstruction affect idle descent trajectory uncertainty, and to assess how this uncertainty propagates to operational metrics such as along-track error, speed deviations, idle descent completion, IAF delay, and loss of separation.

The objective of this thesis is therefore to improve the understanding of idle descent trajectory uncertainty and its operational consequences. By identifying how wind information and VNAV-PATH behaviour influence descent predictability, the research contributes to the assessment of future arrival concepts in which efficient descent operations must be balanced with the demands of safe and predictable traffic management.

The report is structured as follows. Part A presents the scientific paper, which forms the main body of this thesis. Additional results and supporting analyses are provided in Part B. Finally, the original research proposal, which formed the starting point of this thesis, is included in Part C.

Part A

Scientific Paper

TU Delft

Wind Forecast Driven Trajectory Uncertainty in Idle Descents

Y.Q.F. Karelsz
Supervised by Dr.ir. J. Ellerbroek (TU Delft) and F. Dijkstra (LVNL)
Flight Performance & Propulsion, Aerospace Engineering
Delft University of Technology, Delft, The Netherlands

Faculty of Aerospace Engineering, Delft University of Technology
KDC Mainport Schiphol

Abstract—**This paper quantifies how descent wind forecast uncertainty affects VNAV-PATH idle descents and assesses its operational consequences in dense arrival traffic at Amsterdam Airport Schiphol. A 3-DOF point-mass aircraft model is combined with BADA performance data, KNMI GRIB wind forecasts, reconstructed FMS descent wind profiles, and an arrival scenario model. The framework is benchmarked at operational level using pilot-provided FMS descent forecasts and radar-derived wind profiles. The results show that forecast wind error increases with forecast horizon and fewer uplink levels. Wind uncertainty affects VNAV-PATH idle descents both directly, through the along-track wind component, and indirectly, through energy-management errors that appear as speed deviations. In the traffic scenarios, LoS cases are concentrated among aircraft pairs with small planned EAT spacing. LoS pairs also exhibit larger maximum CAS and wind errors, indicating that speed execution errors and wind uncertainty are associated with increased LoS risk. However, increasing the share of aircraft assigned to older forecast horizons does not measurably increase the mean number of LoS cases per scenario, suggesting that aggregate LoS occurrence is mainly governed by traffic geometry and planned spacing. Higher wind errors also increase the likelihood of thrust or spoiler intervention. Within the assumptions of the model, the results support the operational value of refreshing descent wind forecasts before TOD, but show that the benefit of more recent forecast horizons can be partly masked by interpolation errors in the reconstructed FMS wind profile. The results therefore suggest that forecast recency should be evaluated together with wind profile reconstruction accuracy when assessing the potential benefit of improved descent wind uplinks.**

I. Introduction

The aviation industry is growing rapidly, even as it faces increasingly stringent environmental and noise regulations. This growth creates complex challenges for all the stakeholders within the industry. At major hub airports such as Amsterdam Airport Schiphol, these challenges are compounded by dense air traffic, limited runway availability, and complex airspace. To address these issues, the industry has focused on implementing advanced arrival procedures that reduce fuel burn and emissions without compromising safety or capacity [1].

One of the most promising arrival concepts is the Continuous Descent Operations (CDO), in which an aircraft descends continuously from cruise to landing at or near idle-thrust. Within CDO procedures, and idle descent is the most efficient descent method. In this paper, the term idle descent refers specifically to a VNAV-PATH continuous descent operation flown at idle-thrust from top of descent (TOD) to the initial approach fix (IAF). The descent after the IAF is not considered, because aircraft then enter the terminal manoeuvring area (TMA), where vectoring and tactical control actions fall outside the scope of this study. Compared to conventional step-down approaches, idle descents minimize fuel consumption and noise by reducing thrust, level segments, and spoiler deployment. Previous operational trials at Schiphol and other major airports have demonstrated potential fuel savings and notable reductions in noise nuisance for surrounding communities [2], [3]. However, despite these benefits, the large-scale implementation of idle descents during high-traffic periods remains limited.

A key limitation is the reduced predictability of idle descents. Because thrust remains at idle, these trajectories are more sensitive to variations in aircraft mass, atmospheric conditions, and especially wind prediction errors. Even small discrepancies between predicted and actual winds during descent can lead to deviations in speed, altitude, and arrival time, which in turn complicate spacing management in dense terminal airspace [4], [5]. Simulations of idle descents showed improved requested time of arrival (RTA) performance when reducing wind prediction errors [6], [24]. However, these studies only implemented RTA guidance laws. The most efficient descent method, according to *Bronsvoort et al.* [7], VNAV-PATH was not considered. Previous flight trials have used VNAV-PATH, such as Boeing's Oceanic Tailored Arrivals (OTA) at San Francisco [8] and the Tailored Descent Wind experiments at Melbourne [9]. Results showed that improving wind inputs can significantly reduce trajectory uncertainty. Nonetheless, these studies were limited in scale and scope, often based on a single aircraft type or small data sets.

The impact of VNAV-PATH idle descent uncertainty on dense arrival traffic operations remains insufficiently quantified. The main contribution of this paper is a quantitative assessment of idle descent trajectory uncertainty under realistic wind forecast and FMS guidance conditions, and an evaluation of its cumulative operational impact in high-density arrival traffic at Amsterdam Airport Schiphol. This paper is outlined as follows: in section II relevant background knowledge is presented; section III presents the methodology; section IV discusses the hypotheses; section V describes the experimental setup; section VI covers the results; section VII interprets the results.

II. Background

This section presents background information relevant to the methodology of this paper. Information on idle descents and trajectory uncertainties are discussed.

A. Idle Descents

In an idle descent the aircraft descends along a pre-calculated path with thrust set to idle. Depending on the selected Cost Index of the flight, a target Mach and CAS are maintained until speed constraints are encountered, such as the TMA or Altitude speed constraints. In figure 1 an example vertical profile of an idle descent is shown. Although idle descents are the most fuel- and noise- efficient, implementation into daily operations is difficult. During an idle descent no thrust or spoilers can be deployed, as doing so would result in a suboptimal descent. Between the TOD and IAF no flaps are deployed either, leaving only elevator, aileron and rudder authority for control. Therefore, vertical trajectory corrections must be achieved through pitch control which is now directly linked to the velocity, due to the idle thrust setting. This decreases the predictability of the aircraft [10]. Flight tests of idle descents at Schiphol showed 25-40% drop in fuel consumption. However, it was also concluded that additional spacing was required due to the additional trajectory uncertainties [3].

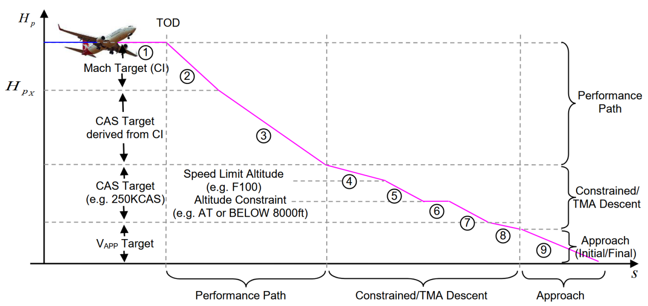

Fig. 1. Example of a vertical profile of an idle descent. [4]

B. Trajectory Uncertainties

An analysis of the impact of the CDO's prediction accuracy was performed by *Raghunandan et al.* [14]. In this study simulations with different prediction accuracies were performed. Results showed a significant improvement in amount of CDO flown when the prediction accuracy was improved. Furthermore, *Blom et al.* [15] found similar results during high traffic density scenarios. Apart from allowing CDO to be flown more often, reducing trajectory uncertainties can also improve the descent efficiency itself. *Fricke et al.* [16] showed that aircraft type, mass and meteorological parameters are vital for designing the optimal descent profile. Hence, understanding the influence of uncertainties in these parameters is important as it impacts descent performance.

The control logic of the aircraft can be adapted to strike a preferred balance between: altitude, speed, and energy efficiency [17]. For example, RTA managed descents try to minimize arrival time errors. However the vertical profile uncertainty can best be reduced by flying a path managed descent instead. This adversely affects the speed and temporal performance of the descent but provides a consistent descent path and is the most economical descent strategy [7].

Ledesma et al. [17] presents a FMS guidance law to maximize IAF arrival time predictability for CDO. It mentions how wind uncertainty will affect aircraft differently depending on type, conditions and guidance law. It tries to minimize the influence of wind, mass and control uncertainties by improving the guidance law. The improved guidance law followed a constant FPA along the CDO for maximum predictability. 3-DOF point-mass simulations of B737-700 were performed starting at 10.000 ft and ending at 2000 ft. Results showed little time deviation due to deviations in wind gradient or weight. However large time deviations due to constant wind error and inaccuracies in the γ execution were found. The study introduced these errors as nominal unknown components, which overestimates the impact of γ execution as this would normally oscillate around a given value. Hence, the findings of this study suggest that wind magnitude uncertainty is the largest contributor to arrival time deviations.

In *Bronsvoort et al.* [18] it was demonstrated that with improved input data for ground trajectory predictors (TP), uncertainties can be reduced. The study added descent schedule data and reduced wind prediction errors by increasing resolution and improving descent wind profile computation. The additional accuracy that was obtained by including the descent schedule is only relevant for improving the predictability of ground TPs. However, the improved temporal accuracy that resulted from using improved wind data is an important finding that highlights the importance of accurate weather data when modeling idle descents.

Uncertainties in wind speeds are especially important since it directly impacts ground velocity, an important parameter for ATC [19], [20]. *E. J. C. Magaña* [20] found a clear correlation between the standard deviation of the along-track wind speed and the ground speed. This correlation can clearly be seen when analyzing the along-track difference of a reference trajectory and actual trajectory. In *Lee et al.* [8] this difference is expressed as:

$$Along\text{-}track\ Error = \sum_{i=1}^{n} [(V_{g\_ref} - V_{g\_actual})\Delta t]_i \quad (1)$$

Here V_{g_ref} and V_{g_test} are the ground speeds for the reference and test trajectories respectively, for example the FMS predicted trajectory and the actually flown trajectory. Substituting V_g for $V_T + V_{Wind}$ and the intended speed schedule ($\sum_{i=1}^{n}[V_T]_i$), yields:

$$Along\text{-}track\ error \approx \sum_{i=1}^{n} [(V_{wind\_ref} - V_{wind\_actual})\Delta t]_i \tag{2}$$

In 2007 operational trials for idle descents were done at San Francisco, called the Oceanic Tailored Arrivals (OTA) trials [21]. Results not only showed a reduction in fuel usage, but also a clear reduction in temporal FMS prediction error after uplinking wind data. A few years after the start of the OTA trials a second study investigated the FMS execution of idle descents using an extended version of the original dataset, still only from a single B777 [22]. The author of this study had performed a similar analysis using a B737 flight simulator a few years earlier in [23]. The intended performance was compared to the actual performance of all suitable descents, comparing the lateral and vertical tracks, airspeeds and IAF crossing times. It was found that the airspeed is usually within 0.01 of the target Mach and within 10 KCAS of the target CAS, which would result in a temporal error between TOD and IAF of about 20-35 seconds. Further analysis of the actual and FMS predicted IAF crossing times showed an even larger error of about 50 seconds. Hence, the paper concludes that about half of this error can be attributed to execution errors of the speed schedule, and the other half to other major sources like descent wind forecast errors. It also stated that the former part of the error can likely not be reduced, which could be explained by limitations of the FMS. This is also supported by *Pradeep et al.* [5], which states that the FMS performance model might not be accurate enough to predict actual aircraft responses in idle-thrust to atmospheric and weather conditions.

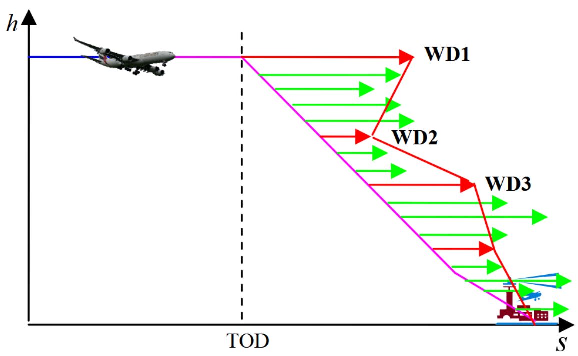

Fig. 2. Descent forecast errors due to the FMS interpolation [9].

The FMS interpolates the descent wind forecast to construct a complete wind profile along its descent path as illustrated in figure 2. The weather forecast and interpolation introduce wind profile errors. Any wind profile errors will result in groundspeed and geometric path errors [9]. This is due to the wind profile affecting the predicted groundspeed, flight path and drift angles, and tail or headwinds. This can be seen in equation (3), the first two components indicate the indirect effect of a change in descent path due to prediction errors and the third indicates component the direct effect of wind prediction error.

$$\begin{aligned}\Delta V_g = &(V_{\mathrm{T}} + \Delta V_{\mathrm{T}}) \cos(\gamma_{\mathrm{a}} + \Delta\gamma_{\mathrm{a}}) \cos(\chi_{\mathrm{dr}} + \Delta\chi_{\mathrm{dr}}) \\ &- V_{\mathrm{T}} \cos\gamma_{\mathrm{a}} \cos\chi_{\mathrm{dr}} + \Delta V_{wind}\end{aligned} \tag{3}$$

Bronsvoort et al. [9] tried to reduce wind profile errors by first applying the planned trajectory to a higher resolution weather forecast grid and re-computing the trajectory according to predicted conditions. Afterwards, the uplinked wind data was tailored to minimize the error between the interpolated weather profile and the base weather prediction profile. Although the study managed to reduce wind prediction errors from planned trajectory deviations and interpolation, the operational impact could not be analyzed due to large forecast errors.

More recent studies have analyzed the effect of wind uplink on the RTA performance. Simulations of different descent forecast level selection methods concluded that uplinking four levels instead of zero yielded significant performance gains ($\pm 50s$) [24]. Further improvements can be made when uplinking nine levels instead of four, although these were of a much smaller magnitude ($\pm 0.5s$). Optimizing the forecast for magnitude performed best, and a large impact on RTA performance by procedural speed constraints was found. Monte Carlo simulations with changing wind permutations for each descent further support these findings [6]. The study concluded that wind forecast errors in magnitude, location and variability have a considerable impact on RTA performance. Furthermore, it was found that FMS RTA capability also has a large impact on the RTA performance. However, it is important to note that both studies only applied RTA FMS logic.

C. Research Gap

Previous studies show that descent wind uncertainty affects idle-descent predictability, that improved wind uplink can reduce arrival-time prediction errors, and that guidance strategy determines how uncertainty appears in the flown trajectory. Point-mass studies such as *Ledesma et al.* [17] provide useful insight into guidance behaviour, but use simplified disturbance representations and do not evaluate VNAV-PATH idle descents under realistic forecast wind fields. Wind uplink studies such as *Reynolds et al.* [6] quantify the effect of forecast quality and uplink resolution, but mainly in terms of RTA performance, trajectory-prediction accuracy, fuel efficiency, or arrival-time error. Moreover, flight-trial analyses indicate that both speed-schedule execution errors and descent wind forecast errors contribute to arrival-time deviations, but these speed deviations have not been propagated to along-track uncertainty and loss-of-separation occurrence (LoS) in dense arrival traffic. It therefore remains insufficiently quantified how wind forecast horizon, FMS wind profile reconstruction, and VNAV-PATH energy-management behaviour jointly affect speed deviations, along-track predictability, idle-descent completion, and conflict occurrence. This study addresses this gap using GRIB-based descent wind forecasts, reconstructed FMS wind profiles, a VNAV-PATH idle-descent simulation model, and Schiphol arrival traffic scenarios with LoS detection.

III. Methodology

The aim of this research is to quantify how descent wind forecast horizon and wind uplink resolution influence idle-descent trajectory uncertainty, and asses the operational consequences of horizon recency. Point-mass aircraft performance simulations of idle-thrust continuous descents are used to evaluate how increasing wind uncertainty affects trajectory predictability, including speed, along-track, and arrival-time errors. The assumed FMS guidance behaviour is included as a sensitivity factor, since it determines how wind induced energy errors are distributed between speed and path deviations in the simulation model. Schiphol is used as a case study and data source, providing representative arrival routes, traffic scenarios, aircraft types, and meteorological conditions. The resulting trajectory uncertainty is then incorporated into an air traffic scenario model to evaluate its impact during high-density arrival operations and to identify implications for operational mitigation. This section presents the overall methodological approach, including the equations of motion, the idle descent simulation framework, underlying assumptions, and operational impact modeling.

A. General Outline

In order to analyze trajectory uncertainties of idle descents a detailed understanding of aircraft performance under idle-thrust conditions is required. While general sources of trajectory uncertainty have been identified in previous research discussed in section II-B, a performance-based analysis of idle descent flight mechanics using VNAV-PATH FMS logic, and its operational implications during high-density arrival scenarios remains limited. To address this gap, a point-mass aircraft model is combined with high-resolution numerical weather forecast data to simulate idle descents from TOD to the IAF (FL100). The simulation framework enables a systematic evaluation of the impact of forecast horizon, wind uplink levels, FMS logic, traffic scenarios and meteorological conditions on trajectory uncertainty. Validation against real flight data is performed to verify that simulated trajectories exhibit realistic magnitudes and trends. The validated idle descent simulations are the basis of the arrival scenario model, allowing the assessment of cumulative effects on arrival operations. In current operations, aircraft may rely on wind data uploaded prior to departure or during cruise. By requiring aircraft to refresh and uplink the most recent forecast shortly before top of descent, forecast errors can be reduced operationally. This study therefore evaluates not only the sensitivity of idle descents to forecast horizon, but also the potential operational benefit of enforcing more recent wind updates prior to descent.

B. Equations of Motion

By deriving the Equations of Motion (EOM) for descents a clear understanding of the flight mechanics that drive trajectory uncertainty can be identified. In figure 3 the free body diagram of an aircraft during its descent is shown. The true airspeed (TAS) magnitude is denoted by V_T, and the aerodynamic Flight-Path Angle (FPA), γ is defined as the angle between the true airspeed vector and the local horizontal. The aerodynamic forces acting on the aircraft are thrust T, drag D, and lift L, while m denotes aircraft mass and g gravitational acceleration. The horizontal velocity component along the flight path is denoted by $V_{horizontal}$ and the vertical velocity component by V_V. Since the wind field is defined in the Earth-fixed frame and the motion equations are expressed in the aerodynamic frame, vertical wind gradients introduce coupling terms between the two frames. The lift, drag, thrust and velocity are derived in the aerodynamic reference frame, in which the X_a-axis is aligned with the true airspeed vector V_T and the Z_a-axis is perpendicular to it. The gravitational forces are illustrated in the Earth-fixed initial frame, which in this case is equal to the aircraft body frame, X_b and Z_b. Additionally, the altitude h and the wind velocity V_{wind} are also defined in this frame.

The following assumptions were made when deriving the equations of motion and the free body diagrams:

- Spherical and non-rotating Earth.
- The aircraft is rigid and symmetric.
- Thrust angle is parallel to the aerodynamic velocity ($\alpha_T = 0$).
- Symmetric flight.
- γ is negative for descent.
- Steady horizontal winds only depending on altitude.
- Small angles.

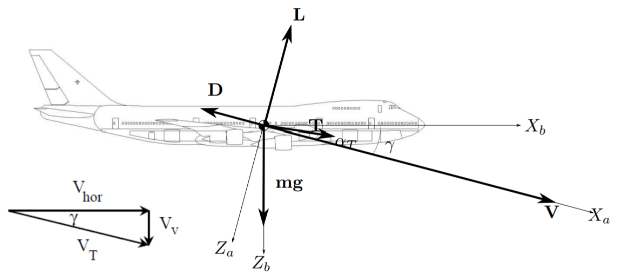

Fig. 3. Free body diagram of the aircraft [11]

Under these assumptions, the equations of motion governing idle descent dynamics can be expressed as follows:

$$m\frac{dV_T}{dt} = T - D - mg\sin\gamma - mV_T\frac{dV_{\text{wind}}}{dh}\sin\gamma\cos\gamma \quad (4)$$

$$mV_T\frac{d\gamma}{dt} = L - mg\cos\gamma + mV_T\frac{dV_{\text{wind}}}{dh}\sin^2\gamma \quad (5)$$

The equations of motion are formulated in the aerodynamic reference frame, X_a, as illustrated in the free body diagram. The equations above are taken from *Pradeep and Wei* [5] and are the equations of motion parallel and perpendicular to the aerodynamic flight path shown in equation (4) and equation (5) respectively. Equation (4) can be derived by equating the acceleration parallel to the aerodynamic flight path to the parallel forces. Equation (5) is derived similarly by equating perpendicular acceleration with forces. Looking at equation (4) under idle-thrust conditions ($T = 0$) shows that the aircraft acceleration is primarily a function of γ, as drag depends on γ and the wind term is negligible under small angles. During a descent the path is controlled by the descent rate and ground velocity, expressed with:

$$\frac{dh}{dt} = -V_T sin\gamma \tag{6}$$

$$V_g = V_T + V_{wind} \tag{7}$$

Combining this with equation (4), shows that altitude corrections have to be performed by changing γ, inherently causing velocity changes. Furthermore, wind disturbances cause errors in ground velocity, which dictates arrival time. Compensating this requires velocity corrections, again by γ control, inducing altitude errors instead. During a normal descent this coupling of errors can be compensated with thrust or spoilers, changing the velocity without affecting the altitude. However, as this is not possible during idle descents speed or path deviations cannot be completely eliminated.

Pradeep and Wei [5] derive an expression for the FPA relative to the ground (γ_g). First the small angle approximation is applied and the time derivatives of true airspeed eliminated in equation 4 yielding:

$$m\frac{dh}{dt}\frac{dV_T}{dh} = T - D - mg\gamma - mV_T\frac{dV_{\text{wind}}}{dh}\gamma \tag{8}$$

From figure 3 the following expression for γ can be derived:

$$\gamma = \frac{V_V}{V_T} = \frac{\frac{dh}{dt}}{V_T} \tag{9}$$

Re-arranging equation 8 and substituting for γ using equation 9 gives:

$$\gamma = \frac{T - D}{\left(mg + mV_T\frac{dV_{\text{wind}}}{dh} + mV_T\frac{dV_T}{dh}\right)} \tag{10}$$

The equation for the FPA relative to the ground (γ_g) is similar to equation 10 with V_T substituted for V_g. Using this and equation 7 the following expression for γ_g is derived:

$$\gamma_g = \frac{T - D}{\left(1 \pm \frac{V_{\text{wind}}}{V_T}\right)\left(mg + mV_T\frac{dV_{\text{wind}}}{dh} + mV_T\frac{dV_T}{dh}\right)} \tag{11}$$

When the aircraft parameters are known the feasible idle descent paths can be constructed from equation (11). Given TOD and IAF altitudes and a 30 second ETO range the resulting flight envelope of an example idle descent can be found in figure 4. Although variations in descent path are still possible by reconfiguring the speed schedule, the flight envelope is greatly reduced compared to conventional step-down procedures. Furthermore, in order to fly the idle descent successfully no ATC intervention can be made after TOD, further restraining flight flexibility.

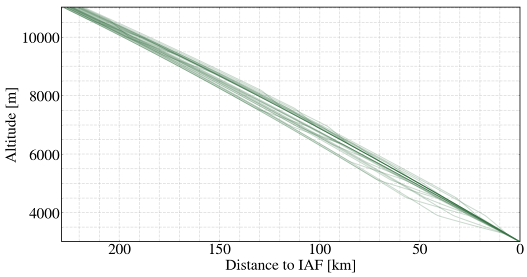

Fig. 4. Feasible idle descent paths within a 30 second ETO range and two constant CAS sections.

C. Aircraft Performance Models

Two aircraft performance models are relevant for this study, the Base of Aircraft Data model and the MITRE point-mass aircraft model.

1) BADA: The Base of Aircraft Data (BADA) contains data and models for specifying operational parameters, procedures and performance for different aircraft [12]. It can serve as a backbone for trajectory simulations and prediction algorithms applied to the Air Traffic Management domain. At the heart of the performance model is the Total Energy Model (TEM):

$$(T - D)V_T = mg\frac{dh}{dt} + mV_T\frac{dV_T}{dt} \tag{12}$$

With equation (12) the forces on the aircraft can be inferred, when given the accelerations of the aircraft. Combined with the performance database and operational constraints, fuel and thrust estimates of trajectories can be made.

2) MITRE Point-Mass Aircraft Model: The MITRE corporation designed a method for 3-DOF point-mass aircraft fast time simulations. It is built upon similar EOM as in III-B, however the symmetric flight assumption is now removed. Hence, roll and heading are introduced as ϕ and ψ respectively. Furthermore, the equations are derived in the Earth-fixed initial frame in order to incorporate wind effects. The wind velocity is divided in its x and y components, V_{wx} and V_{wy}. Since the EOM are dependent on aircraft parameters such as drag- and lift coefficients, the model uses the necessary aircraft parameters from BADA. This results in the following kinematic equations:

$$\begin{aligned} \dot{x} &= V_T\cos\gamma\cos\psi + V_{wx} \\ \dot{y} &= V_T\cos\gamma\sin\psi + V_{wy} \\ \dot{h} &= -V_T\sin\gamma \end{aligned} \tag{13}$$

Which are combined with the following dynamic equations:

$$\begin{aligned} \dot{V}_T &= \frac{T - D}{m} + g\sin\gamma + V_T\left(\frac{\partial V_{wx}}{\partial h}\cos\psi + \frac{\partial V_{wy}}{\partial h}\sin\psi\right)\sin\gamma\cos\gamma \\ \dot{\gamma} &= \frac{-L\cos\phi + mg\cos\gamma}{mV_T} - \left(\frac{\partial V_{wx}}{\partial h}\cos\psi + \frac{\partial V_{wy}}{\partial h}\sin\psi\right)\sin^2\gamma \\ \dot{\psi} &= -\frac{L\sin\phi}{mV_T\cos\gamma} - \left(\frac{\partial V_{wx}}{\partial h}\sin\psi - \frac{\partial V_{wy}}{\partial h}\cos\psi\right)\tan\gamma \end{aligned} \tag{14}$$

The dynamic equations are derived following the point-mass aircraft formulation presented by Weitz [13]. In the model guidance laws are introduced to follow a certain trajectory. Apart from speed control by using thrust, a control logic by adjusting γ is also implemented. For simulating idle descent this control logic is particularly interesting. An Energy Share Factor (ESF) which dictates the ratio of power allocated to changing altitude versus airspeed is introduced. By combining this with the altitude and speed error, the commanded FPA, γ_c and thrust are calculated. The FPA command is then passed onto the model via the FPA rate of change, $\dot{\gamma}$, adjusting the term based on the FPA error and wind-gradient corrections:

$$\dot{\gamma} = k_\gamma \left(\gamma_c - \gamma\right) - \left(\frac{\partial V_{wx}}{\partial h}\cos\psi + \frac{\partial V_{wy}}{\partial h}\sin\psi\right)\sin^2\gamma \quad (15)$$

The thrust and roll angle are also controlled via the respected rate of change and gains:

$$\begin{aligned} \dot{T} &= k_T \left(T_c - T\right) \\ \dot{\phi} &= k_\phi \left(\phi_c - \phi\right) \end{aligned} \quad (16)$$

This ensures realistic aircraft response when the gains are tuned correctly. Furthermore, since this model explicitly resolves speed and flight path it is particularly suitable for trajectory uncertainty analysis.

D. Assumptions

The idle descent simulation framework relies on several assumptions. First, the assumptions used to model the idle descents are covered. Afterwards the additional assumptions needed for the arrival scenario model are discussed.

1) Idle Descent Simulation Assumptions:

- Simulation errors resulting from BADA coefficient inaccuracies, point-mass EOM simplifications, spherical Earth assumptions, or numerical integration methods are negligible relative to wind-induced uncertainties.
- The computed wind field accurately depicts descent wind profiles.
- Indicated airspeed (IAS) is assumed equal to calibrated airspeed (CAS).
- Idle-thrust is assumed constant during the descent.
- CAS deviations are within -15 kt and +10 kt before speed management is engaged [23].

2) Arrival Scenario Model Assumptions:

- ATC has access to ATS B2 ADS-C data, giving ATC insight to descent paths.
- Tuned speed schedules, fixed arrival tracks, and prescribed expected approach times (EATs) represent a hypothetical idle descent traffic scenario.
- No weather avoidance, emergencies or non-nominal procedures are modelled.
- Tactical interventions after TOD are excluded to preserve idle descent completion.
- LoS is only considered between inbound aircraft.
- Future loss-of-separation conflicts are neglected to remove the possibility of false positives, as any ATC intervention would invalidate idle descent execution.
- Pilot execution errors are neglected.
- Aircraft are modeled after the Mach-to-CAS transition.
- Idle descents are executed without airspace constraints.

E. Idle Descent Simulation

Building on the method from *Ledesma et al.* [17] a 3-DOF point-mass aircraft model is employed to analyze idle descents. Aircraft aerodynamic and geometric parameters are obtained from BADA 3, as described in III-C. Thrust is nominally set to idle throughout the descent, except when speed management intervention is triggered. Leaving limited control authority to mitigate disturbances. These disturbances are introduced by the wind model, which is substantially improved compared to *Ledesma et al.* [17] by incorporating real meteorological data. Finally, the FMS algorithm is approximated through an independent path construction and simplified guidance laws, as proprietary FMS algorithms are not publicly available.

1) Idle Descent Path Construction: With equation (11), the idle descent flight path is constructed for each simulated descent. The descent path is computed using aircraft performance parameters, speed schedule and forecast wind levels. Forecast wind levels are selected such that the piecewise-linear wind profile constructed from these levels best approximates the continuous wind field in a least-squares sense [9] [24]. Four or eight forecast wind levels can be used. The descent path is computed backwards from the IAF to cruise altitude.

2) Equations of Motion and Guidance: The actual descent is simulated by integrating the point-mass equations of motion, from section III-C, subject to the realized wind and temperature fields. Deviations from the nominal descent path are corrected using a simplified guidance logic which follows the idle descent path angle γ_{path} and corrects for altitude errors e_h or speed errors e_V. Both error channels are normalized using the altitude and speed gains, K_h and K_V. Furthermore, the energy-share factor (ESF) is implemented to dictate how much each error is corrected which yields the following equation for γ_{cmd}:

$$\gamma_{\text{cmd}} = \gamma_{\text{path}} + \sin^{-1}\left(\frac{(1 - \text{ESF})\, K_h\, e_h - \text{ESF}\, K_V\, e_V}{V_{\text{T}}}\right) \quad (17)$$

In VNAV-PATH ESF=0 and altitude deviations are regulated by pitch commands using equation (15), while speed deviations are allowed to vary within operational bounds before speed management is engaged [24]. When speed deviations exceed allowable bounds, speed management through thrust or spoilers is activated until the speed error has been reduced to 5 kt, and the descent is no longer considered a purely idle-thrust trajectory. The resulting simulation produces a flown trajectory subject to realistic wind-induced deviations.

F. Meteorological Data and Wind Representation

Meteorological data are obtained from GRIB (GRIdded Binary) files provided by the Royal Netherlands Meteorological Institute (KNMI). The data contains hourly forecasts of horizontal wind components and temperature at multiple pressure levels for forecast horizons ranging from 0 to 24 hours. The earliest available forecast (0 h) is treated as the best available representation of actual atmospheric conditions, while remaining forecast horizons are used as predictive wind inputs.

Wind and temperature data are interpolated spatially along the simulated flight path. The accuracy of the wind forecasts is checked with two root mean squared error (RMSE) parameters [6]:

$$\text{RMSE} = \sqrt{\frac{1}{N}\sum_{n=1}^{N}(f_n - o_n)^2} \tag{18}$$

$$\text{RMSVE} = \sqrt{\frac{1}{N}\sum_{n=1}^{N}((u_f - u_o)^2 + (v_f - v_o)^2)} \tag{19}$$

Equation (18) only takes the magnitude of the wind error into account, useful for analyzing separate wind components such as head or cross winds. Equation (19) shows the root mean squared vector error (RMSVE) of the wind direction and magnitude, calculated using both wind vector components.

G. Validation

Validation data were collected for flights that were confirmed by pilots to have been flown in VNAV-PATH during the idle-descent segment. However, flight data recorder data containing the descent wind forecast were not available for this study, as the descent forecast is part of a separate system and is not stored in the recorded flight data. Therefore, for these flights, pilots provided photographs of the descent wind forecast displayed in the FMS, as shown in figure 5. These forecasts contain the wind values available to the aircraft during descent and are therefore representative of the wind information used by the FMS.

The FMS descent forecast was combined with radar data for the corresponding flight to compare the descent wind profile with the encountered wind conditions during the descent. For each validation flight, the forecast wind values were interpolated over the observed descent profile and mapped onto the radar track. Afterwards the along-track descent wind profiles are compared with the encountered along-track wind profile from radar data. This resulted in the total along-track wind RMSE and CAS RMSE over that flight. The validation data are therefore not separated into forecast and interpolation components, but provide an operational reference for the total wind error magnitude observed in real VNAV-PATH descents. Figure 6 shows an example of this comparison for one validation flight. It can be observed that the FMS descent wind profile is similar to the encountered winds.

Because detailed aircraft internal states (e.g., exact mass, angle of attack, proprietary FMS parameters) are not directly observable, validation is conducted at the operational level rather than at the full state level. The objective is therefore not

Fig. 5. Descent forecast validation data.

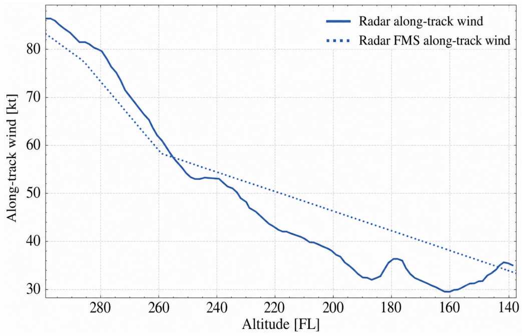

Fig. 6. Along-track wind vs altitude of the descent forecast validation profile and encountered wind profile of a flight fully executed in VNAV-PATH.

to reproduce exact aircraft states, but to reproduce measurable operational outputs. The following observable parameters are compared between simulated and real trajectories:

- Wind RMSE and RMSVE
- CAS deviations
- FPA behaviour

Validation is performed by assessing whether simulated trajectories reproduce the magnitude and statistical distribution of these observed parameters under comparable conditions as the real flights. The model is considered operationally valid if simulated deviations fall within the observed variability range and if the sensitivity to wind forecast errors matches the trends found in real operations.

H. Arrival Scenario Model

The idle descent simulation is integrated into an arrival scenario model to assess the cumulative impact of trajectory uncertainty on arrival operations. A similar method to that used by Reynolds et al. [6] is adopted, now using VNAV-PATH guidance instead of RTA. Representative peak arrival scenarios are imported from Schiphol radar data and reconfigured to support idle descents while retaining the observed lateral routes and scheduling constraints at the IAF. The arrival scenario model combines individual aircraft descent realizations to evaluate operational outcomes such as IAF delay distributions and loss of separation occurrence.

For each scenario, an inbound peak, truth wind field, and forecast horizon distribution are selected. These forecast horizon distributions are intended to represent different operational wind-uplink conditions: a short-biased distribution represents operations where most aircraft receive recent forecast updates, a balanced distribution represents mixed forecast recency, and a long-biased distribution represents less favourable operations in which a larger share of aircraft descends using older forecast information. By sampling a forecast horizon independently for each aircraft, the same traffic scenario can be evaluated under many possible combinations of aircraft-specific forecast horizons, rather than assuming that all aircraft in the scenario use the same forecast horizon. The scenario is then repeated with stochastic forecast horizon assignments until the resulting operational metrics have converged.

The model separates the construction of the planned traffic scenario from the execution of the individual aircraft descents. During the planning stage, idle-descent reference trajectories are generated using the 0 h forecast. This common planning forecast is used to match feasible TOD locations to the observed radar trajectories and to remove pre-existing loss of separation events between planned reference paths. During the execution stage, each aircraft is assigned an individual forecast horizon according to the selected forecast horizon distribution. A new FMS reference path is then constructed using the assigned forecast horizon, while preserving the selected lateral track, speed schedule, and IAF constraints. The aircraft subsequently flies this reference path in the 0 h truth wind and temperature field. The difference between the assigned forecast wind and the truth wind therefore represents the descent execution uncertainty.

1) Descent Path Search: Before the traffic scenario is simulated, idle-descent reference paths are constructed for each flight. For each aircraft, a 60 s estimated-time-over range at the IAF is considered, allowing multiple feasible idle-descent candidates as illustrated earlier in figure 4. Candidate paths are generated backwards from the IAF to the TOD using the 0 h forecast wind field. The vertical profile of each candidate is computed using the idle-descent energy relation in equation (11), together with the aircraft performance model and the selected CAS schedule.

The search considers speed schedules between 230 kt and 320 kt in 5 kt increments, using either one or two constant-CAS segments. For two-segment schedules, the speed change is limited to 10–25 kt and the crossover altitude is varied. Each candidate path defines a planned altitude, speed, groundspeed, and timing profile between TOD and IAF. The resulting TOD location is compared with the observed radar position at the corresponding TOD time. If the distance between the candidate TOD and the radar trajectory is within one nautical mile, the speed schedule is accepted as a realistic idle-descent candidate. If no suitable speed schedule is found, the flight is registered as a non-idle descent and the original radar trajectory is retained in the scenario.

2) Speed Schedule Resolution: Because the constructed idle-descent paths differ from the original radar trajectories, pre-existing LoS cases may be introduced within the realistic idle-descent paths. Before the stochastic execution stage is simulated, these planned paths are checked for LoS occurrence with a simplified AMAN module. If possible, pre-existing LoS are removed by selecting alternative feasible speed schedules from the candidates identified during the descent path search. This step is only used to reduce LoS cases already present in the planned feasible paths, such that remaining LoS cases after simulation can be interpreted primarily as the result of descent execution uncertainty.

3) Idle Descent Simulation: After speed-schedule resolution at the candidate path level, each aircraft is simulated independently. The aircraft type, lateral track, selected speed schedule, and assigned forecast horizon are passed to the idle-descent simulation. A new FMS reference path is constructed using the assigned forecast horizon, while keeping the planning-stage lateral track, speed schedule, and IAF constraints unchanged. The aircraft then follows this FMS reference path in the 0 h truth wind and temperature field. The resulting flown trajectories are combined into a traffic scenario, allowing LoS cases and IAF delay distributions to be evaluated under stochastic wind-forecast uncertainty.

I. LoS Detection

Minimum separation distance violations are detected by comparing the simulated trajectories of inbound aircraft after they have been combined into a single traffic scenario. A loss of separation is registered when the horizontal and vertical separations between an aircraft pair fall below 1000 ft of vertical separation and 5 NM of horizontal. LoS detection is only applied to inbound aircraft included in the arrival scenario.

LoS counts are reported as unique aircraft-pair LoS cases. A loss of separation case is defined as a moment in which two aircraft violate the separation threshold. If the same aircraft pair separates and later violates the threshold again, this is not counted as a new LoS.

J. Statistical Analysis

To assess the stability and interpretation of the stochastic simulation results, additional statistical post-processing was performed on the scenario outputs. For each traffic scenario and forecast distribution case, the mean number of LoS cases, along-track RMSE, CAS RMSE, and wind-error metrics were calculated across the stochastic repetitions. The resulting scenario level means were then used to compare the short-biased, balanced, and long-biased forecast distributions.

For each metric, a 95% confidence interval (CI) was calculated around the estimated mean. These intervals were used to indicate the uncertainty of the mean metric obtained from the finite number of stochastic repetitions. The confidence intervals were therefore used to support the comparison between forecast distributions and wind uplink level cases. Differences between cases were interpreted as meaningful when they were larger than the corresponding CI full width and showed a consistent trend across the analyzed scenarios.

Spearman rank correlations were used to assess monotonic relationships between wind-error, speed-error, and along-track uncertainty metrics. This non-parametric measure was selected because the RMSE distributions are not necessarily normally distributed, the relationships can be nonlinear, and speed-management activation may saturate the CAS response. Due to the large number of simulated descents, the magnitude of the correlation coefficients was used for interpretation rather than the statistical significance of the corresponding p-values.

IV. Hypothesis

It is expected that the descent forecast horizon has significant impact on the trajectory, due to additional uncertainties in wind predictions. Furthermore, this independent variable is manageable during operations by requiring aircraft to use recent wind forecast before descending. Hence, the experimental setup described in section V will test the following assumptions:

H1: Trajectory uncertainty during idle descents is systematically influenced by both wind-uplink uncertainty and the assumed VNAV-PATH guidance behaviour. Longer descent wind forecast horizon and fewer uplink levels are expected to increase trajectory uncertainty. By changing the relative priority assigned to path tracking and speed control, the ESF is expected to influence the CAS error.

H2: In high-density inbound traffic scenarios, increasing the number of aircraft subject to older wind forecasts leads to an increased frequency of LoS cases and IAF delays during idle descents.

V. Experimental Setup

This section describes how the methodology in Section III is instantiated to quantify idle descent trajectory uncertainty and to evaluate its operational consequences. The experimental setup defines the experimental variables, simulation architecture and performance metrics required to evaluate the hypotheses. The experiment runs a factorial design of three inbound peaks, two wind forecast level options, five wind conditions from three separate days and three forecast horizon distributions each with 15 stochastic runs yielding 1350 different scenarios and around 50,000 simulated idle descents. The wind conditions were sampled from three different days, with average winds of 10, 40 and 90 kt. The descent wind forecast horizon is selected as a primary independent variable because it represents a controllable operational parameter. The validation set contains $N = 14$ descents, of which $N = 3$ were confirmed by pilot reports to be flown in VNAV-PATH without thrust or spoiler intervention.

A. Experimental Variables

The experimental variables can be divided into independent, control and dependent variables, which are described below.

1) Independent Variables: A stochastic design is used to evaluate the influence of key variables on idle descent trajectory uncertainty. The independent variables of the experiment are:

- **Descent wind forecast horizon**: 12 h, 6 h, 3 h, 2 h, 1 h and 0 h forecasts.
- **Wind Forecast Levels**: 4 and 8 wind forecast levels.
- **FMS ESF**: ESF = 0, 0.5 and 1 settings on the FMS guidance law.

2) Control Variables: To isolate the effects of the independent variables, the following are held constant across runs:

- Idle thrust setting.
- Aircraft performance.
- Speed management activation logic and limits.
- Descent speed schedules.
- Inbound peak traffic scenarios with fixed arrival tracks and EATs for each peak.
- Representative weather conditions in terms of wind magnitudes and forecast errors.
- Minimum separation distances.

3) Dependent Variables: Trajectory uncertainty is quantified using:

- **CAS deviation** relative to the target schedule.
- **Along-track deviation** relative to the FMS planned descent.
- **Idle descent performance**, measured by the share of descents completed without thrust or spoiler use.
- **Number of LoS** observed in the arrival stream after integrating individual descent realizations.

B. Experimental Architecture

The experiment can be separated into different parts. First the trajectory uncertainty of idle descents is studied. Secondly, sensitivity to different FMS guidance laws is analyzed. Finally, the operational impact is assessed.

1) Trajectory Uncertainty: The first part of the experiment evaluates the sensitivity of individual idle descents to forecast wind uncertainty. For each run, a reference idle-descent path is constructed from the IAF backwards to cruise altitude using the selected forecast wind field and the assigned speed schedule. The actual descent is then simulated using the truth wind field. Differences between the forecast and truth wind fields cause deviations between the predicted and flown trajectory. The trajectory-level results are grouped by forecast horizon and by realized total wind RMSE. Box plots are used to compare the distributions of wind errors, CAS error, and along-track error across forecast horizons.

2) FMS Guidance Sensitivity: The FMS guidance behaviour is represented through the simplified VNAV-PATH control logic described in III. Since proprietary FMS control laws are not available, the ESF is used to represent different balances between path tracking and speed regulation. Lower ESF values prioritize altitude/path tracking, while higher ESF values allocate more of the control response to speed-error correction.

The ESF analysis is not used as a final operational recommendation, but rather as a model-sensitivity and calibration study. It provides insight into the extent to which CAS deviations depend on assumed guidance behavior. The resulting CAS-error distributions are compared with the validation data to assess which guidance setting produces realistic speed-error magnitudes.

3) Operational Assessment: Trajectory uncertainty results are propagated to arrival scenarios by assigning forecast horizons (and other relevant factors) to each aircraft in the scenario. Three inbound peaks were selected for the scenarios, one of which is shown in figure 7.

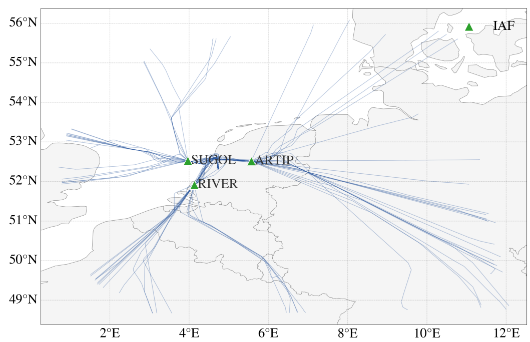

Fig. 7. Radar tracks of one inbound peak.

Each aircraft in the scenario is assigned a forecast horizon stochastically according to a predetermined forecast horizon distribution. Three forecast horizon distributions are used, and can be found in table I. A short-biased, balanced, and long-biased distribution are tested to cover multiple possible distributions since no operational reference data is available. For the speed schedule resolution the 0 h forecast is used in order to minimize ATC error influences. Flights for which no feasible idle-descent schedule is found are retained as radar-based trajectories for traffic and LoS detection completeness but are not included in idle-descent performance statistics. The resulting LoS are analyzed in terms of location, EAT spacing, CAS error and wind errors. In addition, idle-descent performance is evaluated as a function of total wind error to determine whether larger wind errors reduce the probability of completing the descent without speed-management intervention. In figure 8 the structure of the operational assessment is visualized.

TABLE I
FORECAST HORIZON DISTRIBUTIONS USED FOR THE STOCHASTIC SAMPLING.

Distribution	**0 h**	**1 h**	**2 h**	**3 h**	**6 h**	**12 h**
Short-biased	58%	40%	2%	0%	0%	0%
Balanced	20%	15%	15%	20%	20%	10%
Long-biased	0%	0%	7%	24%	43%	26%

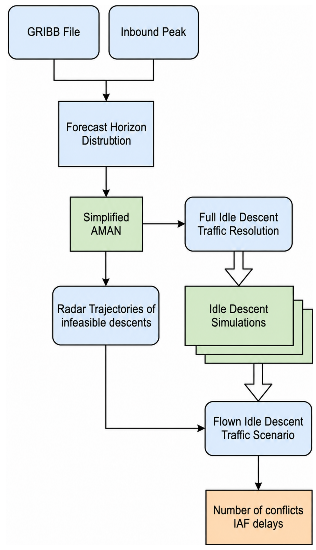

Fig. 8. Single scenario simulation structure.

VI. Results

In this section the results are presented. First the descent wind uncertainty study outcomes are discussed in VI-A. Second, the trajectory uncertainty results are analyzed in VI-B. Third, the FMS guidance sensitivity is covered in VI-C. Finally, the output of the arrival scenario model is presented in VI-D.

A. Descent Wind Uncertainty

The descent wind uncertainty is separated into forecast wind error, interpolation error, and total wind error represented as RMSE or RMSVE in [kt] from equations (18) and (19). The forecast wind error is an uncertainty error, representing the difference between the selected forecast horizon and the 0 h truth wind along the descent trajectory. The interpolation error is a resolution error, representing the difference between the continuous forecast wind field and the reconstructed wind profile obtained from the uplinked wind levels, as illustrated in figure 2. The total wind error combines both effects by taking the difference between the 0 h truth wind and the reconstructed wind profile, therefore representing the wind error in the FMS during descent execution.

For these three types of errors figure 9 shows the along-track wind RMSE in a box plot for the 0 h, 1 h and 6 h horizons when using four level wind uplink. The radar validation points in figure 9 represent the total along-track wind RMSE obtained by comparing pilot-provided FMS descent forecasts with reconstructed along-track wind profiles from the corresponding validation flights. These points therefore provide an operational reference for the total wind-error magnitude, but do not distinguish between forecast horizon and interpolation components.

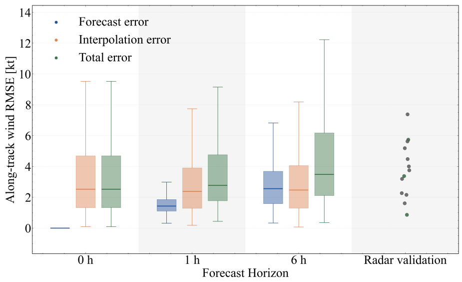

Fig. 9. Forecast, interpolation and total along-track wind error for the 0 h, 1 h and 6 h forecast using 4 wind levels. The radar validation data show the total along-track wind RMSE obtained from pilot-provided FMS descent forecasts and reconstructed wind profiles from validation flights.

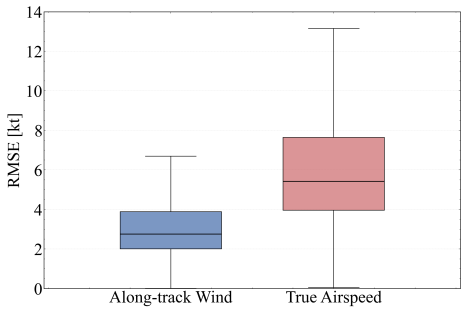

Fig. 11. Box plots of the along track wind error and true airspeed error in kt.

The forecast error component increases with forecast horizon, whereas the interpolation-error component remains comparatively stable across the tested horizons. Consequently, the total wind error also increases slightly after the forecast error has reached a similar magnitude as the interpolation error. This trend occurred across all the horizons, however figure 9 only shows three representative ones. Compared with the radar validation data, the simulated total wind error is similar, indicating that the experiment represents the operational wind-error magnitudes observed in the validation flights.

Figure 10 shows the same along-track wind RMSE box plots for aircraft using eight level wind uplink instead. It can be observed that the interpolation and total errors across the horizons are lower than when using only four wind uplink levels. Furthermore, due to the lower interpolation error, the forecast error affects the total wind error earlier.

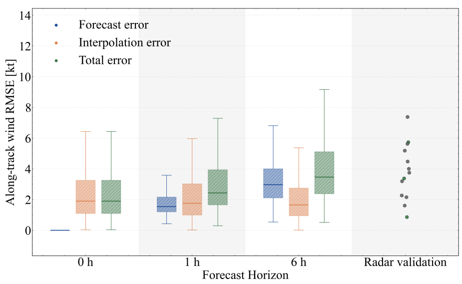

Fig. 10. Forecast, interpolation and total along-track wind error for the 0 h, 1 h and 6 h forecast using 8 wind levels. The radar validation data show the total along-track wind RMSE obtained from pilot-provided FMS descent forecasts and reconstructed wind profiles from validation flights.

B. Trajectory Uncertainty

The trajectory uncertainty of idle descents can be split into two different parts. In equations (1) and (2) the along-track uncertainty was shown to relate to the wind error if the intended speed was flown. However, the along-track uncertainty is not caused by wind error alone. Figure 11 compares the along-track wind-error component with the true-airspeed-error component.

The true-airspeed deviations are larger than the direct along-track wind deviations, showing that deviations from the intended speed schedule are a dominant contributor to ground-speed uncertainty. This indicates that wind uncertainty affects VNAV-PATH idle descents both directly, through the along-track wind component, and indirectly, through energy-management errors that appear as CAS/TAS deviations. The TAS contribution remains dominant, although the relative wind contribution increases with forecast horizon as seen in table II.

TABLE II
MEAN ALONG-TRACK ERROR CONTRIBUTION FRACTIONS BY FORECAST HORIZON.

Horizon	**0 h**	**1 h**	**3 h**	**6 h**	**12 h**
Wind contribution	31.2%	36.9%	37.8%	37.2%	40.5%
TAS contribution	68.8%	63.1%	62.2%	62.8%	59.5%

Figures 12 and 13 show the CAS and along-track RMSE for different total wind errors in 1 kt RMSVE bins. The mean, median and one standard deviation are plotted for each bin. The results show that both CAS RMSE and along-track RMSE increase with total wind error. This indicates that larger total wind errors lead to a measurable degradation in trajectory predictability, reducing the aircraft's ability to remain close to the intended CAS schedule and along-track position. The increase in CAS RMSE is consistent with the path-managed idle-descent formulation, where wind-induced energy deviations are expected to appear primarily as speed deviations when the vertical path is maintained. The observed relationship therefore characterizes how this expected response scales with increasing wind error.

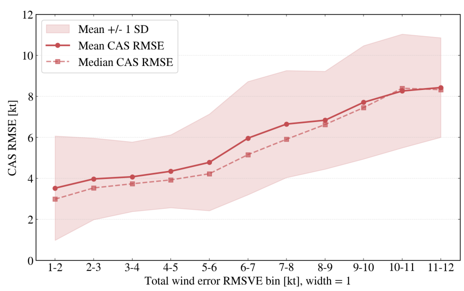

Fig. 12. CAS error for different total wind errors in 1 kt RMSVE bins.

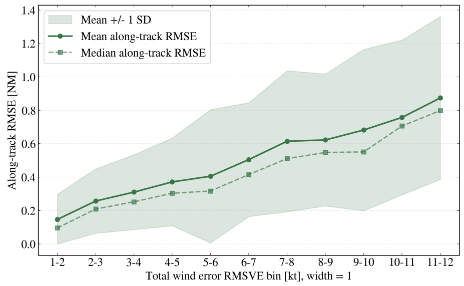

Fig. 13. Along-track error for different total wind errors in 1 kt RMSVE bins.

C. FMS Guidance Sensitivity

Precise FMS guidance laws are proprietary, however they are a vital part of the aircraft performance. Therefore, descents with different ESF settings were tested to analyze the potential impact of the FMS. Figure 14 compares the CAS-error distributions for different ESF settings. The CAS RMSE is plotted for ESF 0, 0.5 and 1 settings alongside the radar validation points.

The ESF parameter in equation (17) determines the relative priority between path tracking and speed-error correction in the simplified guidance law. As expected, increasing the ESF reduces CAS deviations because a larger part of the commanded flight-path-angle correction is allocated to speed regulation.

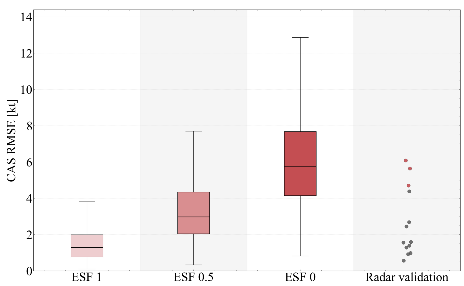

Fig. 14. CAS RMSE for ESF 0, 0.5 and 1 settings. The radar validation points show the CAS RMSE obtained from validation flights.

The comparison with the validation data shows that the apparent best-fitting ESF depends on which validation flights are considered. When all validation points are included, the intermediate ESF setting gives CAS-error magnitudes closest to the observed distribution. However, the confirmed full idle VNAV-PATH descents without thrust or spoiler intervention are more consistent with the $ESF = 0$ setting. This supports the use of ESF = 0 as the baseline VNAV-PATH representation, while the other ESF settings are retained as sensitivity cases.

D. Operational Impact

The operational impact of idle-descent execution uncertainty is evaluated by combining the individually simulated descents into arrival scenarios. As discussed in section V, each scenario consists of one inbound peak, one 0 h truth atmosphere, and one stochastic forecast horizon distribution. Before execution, speed-schedule resolution is applied to reduce LoS occurrence between the planned idle-descent trajectories. The remaining LoS cases therefore represent cases caused by descent execution uncertainty and limited schedule-resolution authority.

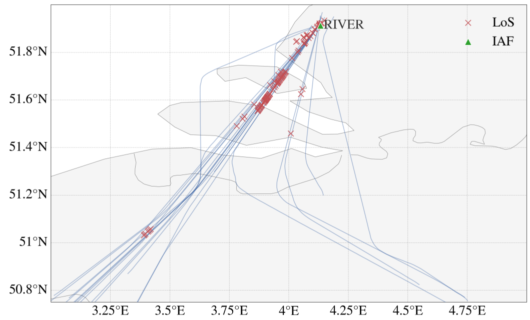

Fig. 15. Radar tracks through RIVER with LoS markers of one scenario.

Figure 15 shows the location of detected LoS cases for one RIVER arrival scenario. LoS occurs along the route and are not limited to the IAF region. This indicates that uncertainty in idle-descent execution can affect spacing throughout the descent, rather than only at the final metering fix.

Figure 16 shows the relation between LoS occurrence and EAT spacing in a complementary cumulative distribution function (CCDF). The CCDF gives, for each spacing value on the horizontal axis, the fraction of aircraft pairs with a larger spacing than that value. The curve for the LoS pairs drops rapidly with increasing EAT spacing, showing that LoS is concentrated among aircraft pairs that were planned close together in time. Once the planned spacing exceeds approximately 2.5 min, the number of LoS cases approaches zero. This confirms that planned arrival spacing remains a driver of LoS risk in dense idle-descent scenarios.

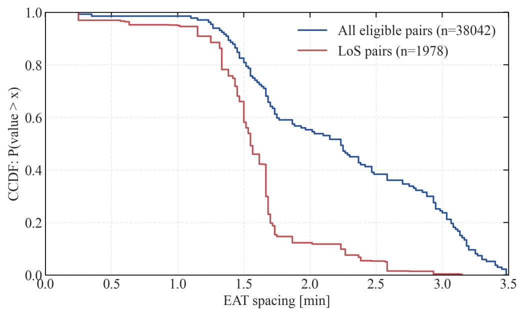

Fig. 16. CCDF of the relative EAT spacing for LoS aircraft pairs and all eligible pairs, showing the fraction of pairs exceeding each spacing value on the horizontal axis, $P(value > x)$.

Figure 17 analyses whether CAS deviations are associated with higher LoS risk. For each aircraft pair in the scenario, the maximum CAS RMSE of the two paired aircraft is assigned to the pair, assuming that the aircraft with the larger speed deviation is the dominant contributor to the spacing error. The ECDF shows the fraction of pairs with a maximum CAS

RMSE less than or equal to each value on the horizontal axis for LoS and non-LoS aircraft pairs. The rightward shift of the LoS-pairs curve relative to the non-LoS-pairs curve indicates that LoS occurs more often in pairs where at least one aircraft has a large CAS deviation. This suggests that speed-execution errors are associated with increased LoS risk, because larger CAS deviations translate into along-track errors.

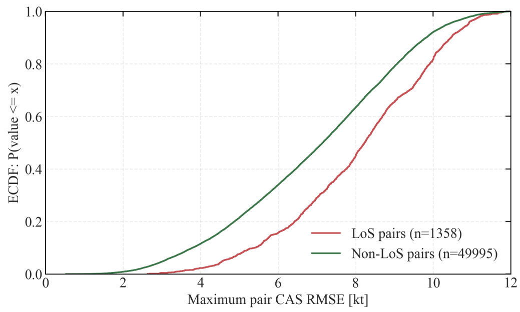

Fig. 17. ECDF of the maximum CAS RMSE for LoS and non-LoS aircraft pairs. The ECDF shows the fraction of pairs with values less than or equal to each maximum CAS RMSE value.

Furthermore, figure 18 presents the same comparison between LoS and non-LoS pairs for the maximum total wind error within each aircraft pair. The LoS-pairs distribution is shifted toward larger wind errors compared with the non-LoS-pair distribution, indicating that aircraft pairs affected by larger wind errors are more prone to lose minimum separation. This is consistent with the trajectory-level results, where larger wind errors were shown to increase CAS and along-track errors. However, the results in Figures 17 and 18 should be interpreted as associations rather than direct causal effects, because LoS occurrence also depends on planned spacing, route geometry, and local traffic density.

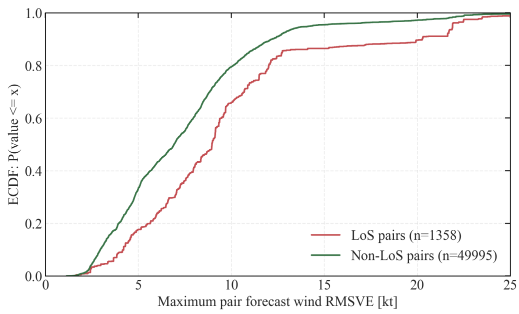

Fig. 18. ECDF of the maximum total wind RMSVE for LoS aircraft pairs and non-LoS pairs. The ECDF shows the fraction of pairs with values less than or equal to each maximum total wind RMSVE value.

IAF delay was also evaluated as an additional operational metric. No systematic increase in absolute IAF delay was observed with increasing total wind error or with forecast horizon distribution. This can be explained by the endpoint nature of the metric: positive and negative wind- and speed-induced timing deviations can partially cancel over the descent before resulting in a final IAF arrival-time error. Therefore, total wind error and forecast horizon affect the local trajectory uncertainty more clearly than the IAF delay.

Figure 19 shows the use of thrust and spoilers as a function of total wind error. The descents are distributed among total wind RMSVE bins of 2.5 kt, and each bin shows the percentage of descents with spoiler, thrust or spoiler and thrust deployment. The probability of speed-management intervention increases sharply once the total wind error exceeds approximately 5 kt. Thrust is used more frequently than spoilers, indicating that aircraft are more often energy-deficient than energy-excessive under the tested conditions. For wind errors above approximately 10 kt, most descents require either thrust or spoiler intervention, although these bins contain fewer samples and should therefore be interpreted with care.

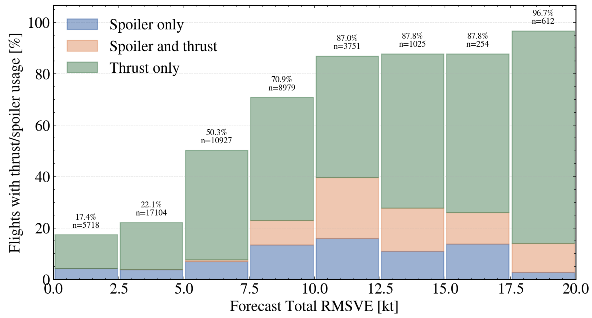

Fig. 19. Speed management intervention rate at different wind errors with the percentage and total flight count of each bin shown.

E. Statistical Analysis

The strongest statistical relation was found between total wind error and along-track error shown in figure 13. For all descents, the Spearman correlation was $\rho_s = 0.876$. This strong association is expected, because an error in the along-track wind component directly affects the ground-speed profile used during the descent. Wind errors therefore translate directly into differences in along-track position and arrival timing.

The relation between total wind RMSVE and CAS error, in figure 12, was weaker. For all descents, the Spearman correlation was $\rho_s = 0.483$. This weaker relation should be interpreted in the context of the implemented VNAV-PATH guidance logic. In the model, VNAV-PATH prioritizes vertical path tracking rather than speed-error correction. As a result, wind-induced energy errors introduce CAS deviations, but these are also partly absorbed through speed changes and speed-management logic. The moderate correlation between wind error and CAS error is therefore consistent with the implemented guidance behaviour.

To analyze the effect of the forecast distribution, the number of LoS cases and the mean along-track RMSE, CAS RMSE, and wind errors of the aircraft, were calculated across three forecast distributions. In addition, the 95% CI full width of each metric was calculated. Differences between forecast distributions were interpreted as meaningful when they exceeded the uncertainty indicated by the CI of the scenario means and showed a consistent trend across the scenarios.

A clear increase in along-track RMSE is observed when older forecast horizons are used more frequently. The forecast and total wind errors also increases for forecast distributions with a larger share of older horizons. Additionally, decreasing the number of descent wind uplink levels from eight to four increases the along-track RMSE for all forecast distributions. These increases in along-track and wind errors caused by older forecast distributions and by using less wind uplink levels are larger than the 95% CI full width. This indicates that these effects exceed the stochastic spread within the scenarios.

The CAS RMSE shows a similar, but weaker, trend. On average, CAS RMSE increases when older forecast horizons are used more frequently. However, the differences between forecast distributions are small compared with the uncertainty of the mean.

The number of LoS cases shows no systematic trend with forecast horizon distribution. Across all three distributions, the mean number of LoS cases is approximately two per scenario, with a CI width of 0.5 LoS cases. Since LoS counts are integer valued, this relatively small interval indicates that the number of LoS occurrences is largely consistent across the forecast horizon distributions.

The results suggest that improved descent winds in the FMS, by using more recent forecast horizons or more uplink levels, reduces trajectory uncertainty. However, the total number of LoS cases was not measurably reduced by forecast horizons or uplink levels, indicating that LoS occurrence is mainly governed by traffic geometry and planned EAT spacing.

VII. Discussion & Conclusion

This section discusses the key findings of the results, and future work on the subject and finally presents the conclusion of the study.

A. Key Findings

The results provide partial support for the hypotheses stated in Section IV. Hypothesis **H1** stated that idle-descent trajectory uncertainty is influenced by wind uncertainty and by the assumed VNAV-PATH guidance behaviour. The first hypothesis is supported within the tested conditions: the total wind error increased with forecast horizon and fewer uplink levels, and total wind error was strongly associated with along-track predictability. However, forecast horizon had little impact on four uplink level descents. Furthermore, the ESF setting had a large impact on the CAS error. Additionally, higher total wind errors are also slightly associated with higher CAS errors. And these speed deviations have a significant impact on along-track uncertainty.

The second hypothesis is partially rejected. Hypothesis **H2** stated that, in high-density inbound traffic scenarios, increasing the number of aircraft subject to older forecasts would increase the frequency of LoS cases and IAF delays during idle descents. LoS cases were associated with higher CAS and wind errors. And the use of older forecast horizons increased the mean along-track error within a scenario. Additionally, higher total wind error increases the speed management intervention rate.

However, increasing the share of aircraft assigned to older forecast horizons did not increase the mean number of LoS per scenario and no systematic effect on IAF delay was observed.

Therefore, the scenario results suggest that forecast uncertainty mainly affects trajectory predictability and idle-descent completion, while aggregate LoS occurrence is likely primarily governed by traffic geometry and planned spacing.

Overall, the results show the importance of speed adherence and forecast accuracy for dense idle-descent operations, since LoS cases are associated with higher CAS and wind errors. Furthermore, larger wind errors increase the frequency of spoiler and thrust deployment during the descents.

B. Discussion

The results indicate that the operational value of more recent descent wind forecasts depends not only on forecast age, but also on how the FMS wind profile is reconstructed from the wind uplink. In the four level wind uplink case, interpolation error formed a relatively large part of the total wind error, which partly masked the benefit of using shorter forecast horizons. The eight level case reduced this reconstruction error and made the influence of forecast horizon more visible in the total wind error. The findings of this study should therefore be interpreted as a result of the combined forecast and reconstruction method applied here, rather than as a general statement about proprietary FMS descent wind profile logic.

A clear correlation between the along-track error and total wind error was found, however this was not the case for the CAS error. This is likely caused by the spoiler and thrust deployment and speed changes limiting the speed errors.

At traffic-scenario level, LoS is associated with small EAT spacing and increased CAS and wind errors. This confirms earlier findings of larger spacing buffers required for idle-descent operations. However, reducing CAS and wind errors can likely further mitigate LoS occurrence and support more predictable use of idle descents in dense traffic. No clear increase in LoS occurrence was observed between the different forecast horizon distributions, which shows that the traffic geometry and planned spacings are still the dominant drivers for aggregate LoS occurrence. Finally, no systematic effect of forecast horizon on IAF delay was found. Likely due to speed and wind errors averaging out throughout the descent, irrespective of magnitude.

These findings should be interpreted within the limitations of the model:

- The shortest forecast horizon is used as a truth proxy rather than measured atmospheric truth. This could have caused conservative wind error values since real atmospheric conditions are more volatile. Furthermore, limited wind conditions were tested.
- The FMS guidance law is simplified and represented through the ESF setting, while actual proprietary VNAV

behaviour is more advanced and differs by aircraft type. Additionally, aircraft performance and proprietary FMS uncertainties remain simplified.
- The validation data set is limited, especially for confirmed fully idle descents.
- The arrival scenario excludes tactical ATC interventions, outbound traffic, weather avoidance, and pilot execution errors.

The trajectory uncertainty results therefore represent a controlled estimate of idle descent uncertainty rather than a full operational performance assessment. The LoS results should therefore be interpreted as operational risk within a simplified scenario model, rather than as a full operational safety assessment.

C. Future Work

Future work should first improve the atmospheric truth representation used in the experiment. In this study, the shortest available forecast horizon was used as a proxy for the realized atmosphere, which might lead to conservative wind-error magnitudes. Comparing the simulation framework against measured descent winds or adding wind gusts would provide a more representative estimate of operational wind uncertainty.

Second, the FMS wind profile reconstruction logic should be made more advanced by using for example, wind blending methods that incorporate current wind measurements into the algorithm.

Third, the validation data set should be expanded. Only a limited number of descents were confirmed to be fully flown in VNAV-PATH without thrust or spoiler intervention. Additional validation flights, ideally from FDR data including aircraft type, FMS mode, descent wind uplink, speed schedule, and intervention status, would allow the simplified guidance model to be calibrated more robustly.

Fourth, the arrival-scenario model should be extended to a wider range of traffic and weather conditions. The present experiment uses a limited number of inbound peaks and wind situations. Testing additional traffic geometries, IAF combinations, wind directions, and wind-shear cases would help determine whether the observed LoS behaviour generalizes beyond the selected Schiphol scenarios.

Finally, future work should include more detailed operational decision logic. The current scenario model excludes tactical ATC interventions, outbound traffic, weather avoidance, and pilot execution errors. Including these elements would move the framework from a controlled uncertainty study toward a more complete operational safety and feasibility assessment.

D. Conclusion

This paper developed and applied a simulation framework to quantify VNAV-PATH idle-descent trajectory uncertainty and its operational impact in dense Schiphol arrival scenarios. A 3-DOF point-mass aircraft model was combined with GRIB-based wind forecasts, reconstructed FMS wind profiles and descent paths, and an idle descent arrival-scenario model with speed-schedule resolution. The model reproduced comparable wind and CAS-deviation mechanisms, although validation was very limited.

The results indicate that larger descent wind forecast horizons and fewer wind uplink levels increase wind error and that this uncertainty propagates into CAS deviations during idle descent. The CAS deviations form an important indirect mechanism through which wind uncertainty affects along-track predictability. In the traffic scenarios, LoS occurs mainly for tightly spaced aircraft pairs, and within the conflicting aircraft at least one aircraft in the pair exhibits larger CAS or wind errors, suggesting an increased LoS risk in these aircraft. Higher wind errors also reduce the probability of completing the descent without thrust or spoiler intervention. The use of older forecast horizons increased the mean along-track error within a scenario. However, increasing the share of older forecast horizons did not affect the aggregate number of LoS cases or IAF delays in the current scenario model.

Within the assumptions of the model, the results support the operational value of reducing descent wind uncertainty before TOD. More recent descent wind forecasts can improve trajectory predictability and reduce the likelihood of speed-management intervention, particularly when the FMS wind profile is reconstructed with sufficient uplink resolution. The results therefore suggest that forecast recency should be evaluated together with wind profile reconstruction accuracy when assessing the potential benefit of improved descent wind uplinks. In dense arrival traffic, such wind information improvements should be considered alongside intent sharing and operational planning, since VNAV-PATH speed uncertainty and planned spacing remain important drivers of LoS occurrence.

REFERENCES

[1] AMS Schiphol, *Flying More Efficient*, Schiphol Group, Amsterdam, The Netherlands, 2025. Available: https://www.schiphol.nl/en/sustainability/in-the-air/flying-more-efficiently-at-schiphol/

[2] Inaad, M., *Fuel and Emission Benefits for Continuous Descent Approaches at Schiphol*, Master's Thesis, Delft University of Technology, Delft, The Netherlands, July 2016.

[3] Wubben, F. J. M., and Busink, J. J., *Environmental Benefits of Continuous Descent Approaches at Schiphol Airport Compared with Conventional Approach Procedures*, Tech. Rep. NLR-TP-2000-275, National Aerospace Laboratory (NLR), Amsterdam, The Netherlands, May 2000.

[4] Bronsvoort, J., Huynh, T., and Enea, G., "An operator-focussed metric for measuring predictability and efficiency of descent operations," *Proceedings of the AIAA Aviation Technology, Integration, and Operations Conference*, Washington, D.C., June 2016. doi:10.2514/6.2016-4219.

[5] Pradeep, P., and Wei, P., "Predictability, variability, and operational feasibility aspects of continuous descent approaches," *Proceedings of the IEEE Aerospace Conference*, Big Sky, MT, Mar. 2017. doi:10.1109/AERO.2017.7943728.

[6] McPartland, M., and Reynolds, T. G., "Exploring wind information requirements for four-dimensional trajectory-based operations," *Proceedings of the USA/Europe Air Traffic Management Research and Development Seminar*, MIT, Cambridge, MA, June 2015.

[7] Bronsvoort, J., et al., "Understanding time-drift for different aircraft descent guidance strategies," *Proceedings of the ATACCS Conference*, London, UK, 2012.

[8] Lee, A., et al., "Performance of trajectory models with wind uncertainty," *Proceedings of the AIAA Modeling and Simulation Technologies Conference*, Chicago, IL, Aug. 2009. doi:10.2514/6.2009-5834.

[9] Bronsvoort, J., et al., "Enhanced descent wind forecast for aircraft," *Proceedings of the USA/Europe Air Traffic Management Research and Development Seminar*, Berlin, Germany, June 2011, pp. 1–10.

[10] Iwata, D., Nonaka, Y., and Itoh, E., "Air traffic control method for more fuel-efficient arrivals in terminal airspace," *Journal of Air Transport Management*, Vol. 128, 2025, p. 102799. doi:10.1016/j.jairtraman.2025.102799.

[11] Sopjes, R., et al., "Continuous descent approaches with variable flight-path angles under time constraints," *Proceedings of the AIAA Guidance, Navigation, and Control Conference*, Portland, OR, Aug. 2011. doi:10.2514/6.2011-6219.

[12] EUROCONTROL Experimental Centre, *User Manual for the Base of Aircraft Data (BADA)*, Rev. 3.6, EEC Note No. 10/04, July 2004.

[13] L. A. Weitz, *Derivation of the Point-Mass Aircraft Model Used for Fast-Time Simulation*, MITRE Technical Report PR-15-1318, McLean, VA, USA, Apr. 2015.

[14] Raghunandan, M., *Evaluating the Impact of Prediction Accuracy on Continuous Descent Operations: The Added Value of Trajectory Predictor Performance Through Air-Ground Datalink*, Master's Thesis, Delft University of Technology, Delft, The Netherlands, Feb. 2024.

[15] Blom, L. M. M., *Investigating Per-Flight Criteria for the Application of Idle and Fixed-FPA Descents Towards the IAF*, Master's Thesis, Delft University of Technology, Delft, The Netherlands, Dec. 2025.

[16] Fricke, H., Seiß, C., and Herrmann, R., "Fuel and energy benchmark analysis of continuous descent operations," *Air Traffic Control Quarterly*, Vol. 23, No. 1, 2015, pp. 83–108. doi:10.2514/atcq.23.1.83.

[17] Gomez Ledesma, R., and Navarro, F. A., "Continuous descent approaches for maximum predictability," *Proceedings of the IEEE/AIAA Digital Avionics Systems Conference*, Dallas, TX, Oct. 2007. doi:10.1109/DASC.2007.4391871.

[18] Bronsvoort, J., et al., "Impact of data-link on ground-based trajectory prediction accuracy for continuous descent arrivals," *Proceedings of the AIAA Modeling and Simulation Technologies Conference*, Boston, MA, Aug. 2013. doi:10.2514/6.2013-5068.

[19] Chaloulos, G., and Lygeros, J., "Effect of wind correlation on aircraft conflict probability," *Journal of Guidance, Control, and Dynamics*, Vol. 30, No. 6, 2007, pp. 1742–1752. doi:10.2514/1.28858.

[20] Casado Magaña, E. J., *Trajectory Prediction Uncertainty Modelling for Air Traffic Management*, Ph.D. Thesis, University of Glasgow, Glasgow, UK, 2016.

[21] Coppenbarger, R. A., and Mead, R. W., "Field evaluation of the tailored arrivals concept for datalink-enabled continuous descent approach," *Proceedings of the AIAA Aviation Technology, Integration, and Operations Conference*, Belfast, Northern Ireland, 2007.

[22] Stell, L., "Flight management system execution of idle-thrust descents in operations," *Proceedings of the IEEE/AIAA 30th Digital Avionics Systems Conference*, Seattle, WA, Oct. 2011. doi:10.1109/DASC.2011.6095979.

[23] Stell, L., "Flight management system prediction and execution of idle-thrust descents," *Proceedings of the IEEE/AIAA 28th Digital Avionics Systems Conference*, Orlando, FL, Oct. 2009. doi:10.1109/DASC.2009.5347570.

[24] Jones, J., et al., "Methods of selecting forecast winds for flight management systems to support four-dimensional trajectory-based operations," *Proceedings of the AIAA Aviation Technology, Integration, and Operations Conference*, Washington, D.C., June 2016. doi:10.2514/6.2016-4069.

Part B

Appendices

TUDelft

A Mass-Error Sensitivity Analysis

An additional sensitivity analysis was performed to evaluate whether uncertainty in the aircraft mass definition affected the descent performance metrics used in this study. Aircraft mass is a relevant parameter for idle descent prediction, since it changes the energy balance and therefore the descent distance required to satisfy a fixed speed and altitude constraint. *Laurel Stell* [37] showed this effect in a B737-700 commercial-FMS simulator study, where aircraft weight was varied together with descent speed and wind conditions. In that study, an increase in aircraft weight of 10,000 lb shifted the FMS-computed top of descent approximately 4.6 NM farther from the meter fix. This confirms that aircraft mass can affect TOD placement and motivates including a mass-error sensitivity check.

In the present simulation, the actual aircraft mass was varied within a prescribed mass range of 5% around the reference value. The reference mass used by the trajectory predictor was then offset by 0%, 25%, or 50% of this prescribed mass variation range. These cases therefore correspond to no reference mass error, a 1.25% mass error, and a 2.5% mass error relative to the nominal aircraft mass, respectively. The mass error cases were evaluated for all forecast horizons using four wind uplink levels to determine whether imperfect mass knowledge materially changed the CAS and along-track trajectory errors.

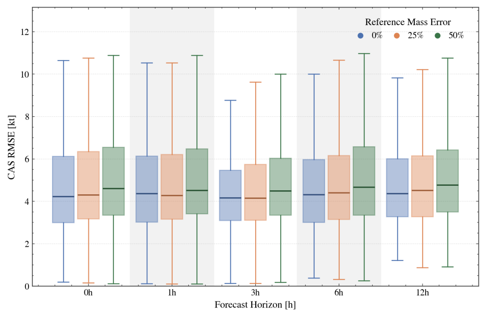

(a) Effect of reference-mass error on CAS RMSE for each forecast horizon.

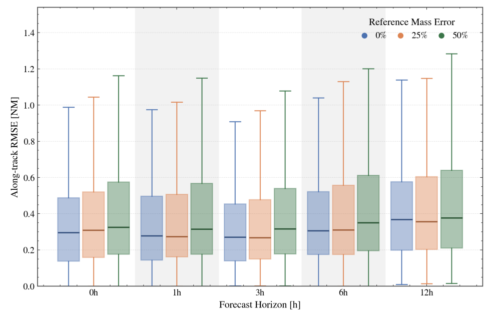

(b) Effect of reference-mass error on along-track RMSE for each forecast horizon.

Figure A.1: Effect of reference-mass error on CAS and along-track RMSE. The mass-error levels are defined relative to the 5% mass-variation range used in the simulation.

The results in Figure A.1a and Figure A.1b show only a small sensitivity to the imposed reference mass error. For CAS RMSE, the median error increases slightly when the reference-mass error is increased, but the distributions largely overlap for the 0%, 25%, and 50% cases at each forecast horizon. The same behaviour is observed for along-track RMSE: the 50% mass-error case generally gives the largest median error, but the shift is small compared with the spread of the distributions and with the differences associated with wind-error variability. While aircraft mass is relevant for TOD placement and idle-descent prediction, the imposed mass errors of 1.25% and 2.5% do not materially change the CAS RMSE or along-track RMSE results. The main uncertainty effects reported in the paper are therefore not driven by the assumed mass variation, but primarily by wind-related uncertainty and the resulting VNAV-PATH energy-management response.

B Statistical Analysis

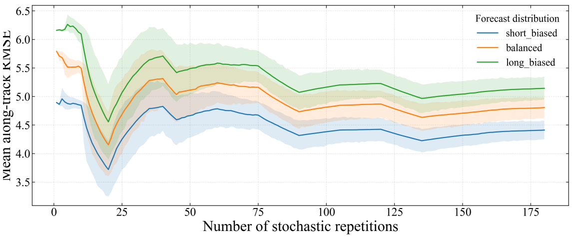

(a) Mean along-track RMSE per aircraft and 95% CI.

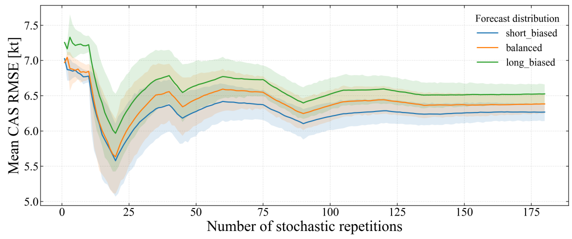

(b) Mean CAS RMSE per aircraft and 95% CI.

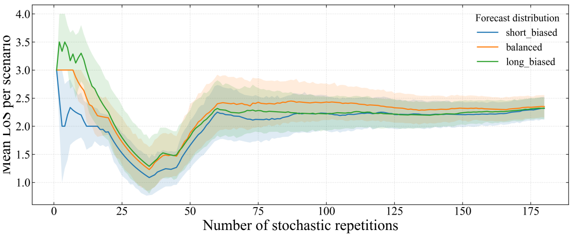

(c) Mean LoS cases per scenario and 95% CI.

(d) Mean total wind RMSE per aircraft and 95% CI.

Figure B.1: Evolution of mean trajectory, speed, separation, and total wind-error metrics with increasing number of scenarios and stochastic repetitions using four wind uplink levels.

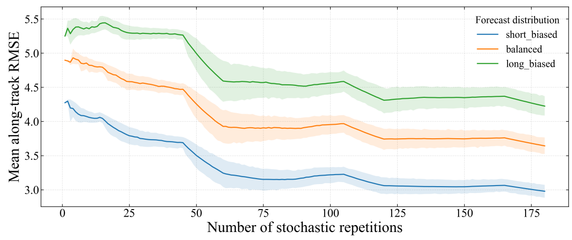

(a) Mean along-track RMSE per aircraft and 95% CI.

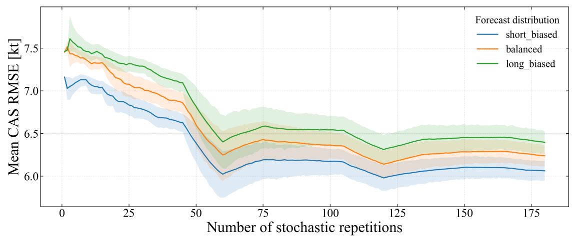

(b) Mean CAS RMSE per aircraft and 95% CI.

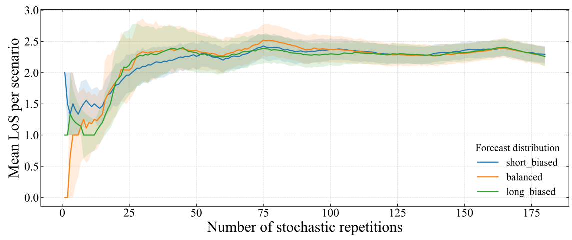

(c) Mean LoS cases per scenario and 95% CI.

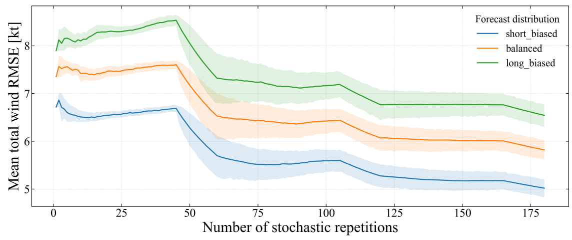

(d) Mean total wind RMSE per aircraft and 95% CI.

Figure B.2: Evolution of mean trajectory, speed, separation, and total wind-error metrics with increasing number of scenarios and stochastic repetitions using eight wind uplink levels.

Part C

Research Proposal

TUDelft

1 Introduction

The aviation industry is growing rapidly, even as it faces increasingly stringent environmental and noise regulations. This growth creates complex challenges for all the stakeholders within the industry. At major hub airports such as Amsterdam Airport Schiphol, these challenges are compounded by dense air traffic, limited runway availability, and complex airspace interactions. To address these issues, the industry has focused on implementing advanced arrival procedures that reduce fuel burn and emissions without compromising safety or capacity [32].

One of the most promising arrival concepts are the Continuous Descent Operations (CDO), in which an aircraft descends continuously from cruise to landing at or near idle thrust. Compared to conventional step-down approaches, CDO minimize fuel consumption and noise by reducing thrust, level segments, and spoiler deployment. Previous operational trials at Schiphol and other major airports have demonstrated potential fuel savings of 25–40% per descent and notable reductions in noise nuisance for surrounding communities [18, 40]. However, despite these environmental and operational benefits, the large-scale implementation of CDO during high-traffic periods remains limited.

A key limitation is the reduced predictability of idle thrust continuous descents (simply called idle descents). Because thrust remains at idle, these trajectories are more sensitive to variations in aircraft mass, atmospheric conditions, and especially wind prediction errors. Even small discrepancies between predicted and actual winds during descent can lead to deviations in speed, altitude, and arrival time, which in turn complicate spacing management in dense terminal airspace [6, 28]. Previous flight trials, such as Boeing's Oceanic Tailored Arrivals (OTA) at San Francisco [12] and the Tailored Descent Wind experiments at Melbourne [7], have shown that improving wind inputs can significantly reduce trajectory uncertainty. Nonetheless, these studies were limited in scale and scope, often based on a single aircraft type or small data sets.

To address this gap, this research will analyze real Flight Data Recorder (FDR) and Flight Management System (FMS) wind-uplink data from multiple KLM (Royal Dutch Airlines) aircraft types operating at Schiphol. By correlating uplinked and realized wind profiles with observed deviations in speed, time, and fuel use, the study aims to quantify how wind-prediction errors and other additional parameters affect the efficiency and predictability of idle descents under operational conditions. In doing so, it will provide new insights into the factors that limit idle descent predictability and offer guidance on how these uncertainties can be managed through improved wind data and trajectory modeling.

The report is structured as followed. In Appendix 2 information about Schiphol Airport and the surrounding Air Traffic Management(ATM) structure are provided. Appendix 3 dives into the definitions and basic principles of CDO. This is followed by a thorough analysis of idle descent predictability in Appendix 4. Afterwards the research foundations are presented in Appendix 5. Finally, in Appendix 6 the methodology and planning is covered.

2 Schiphol Airport & ATM

In this chapter the Schiphol Airport and ATM structure around Schiphol are briefly covered. In section 2.1 Schiphol Airport is introduced. Afterwards the ATM structure around Schiphol is explained in section 2.2.

2.1 Schiphol Airport

Schiphol is one of the busiest airports in Europe, transporting over 60 million passengers and 1.5 million tons of cargo yearly. Furthermore, over 30% of the passengers are transfer passengers increasing operation complexity [31]. To safely transport these passengers, LVNL (Air Traffic Control the Netherlands) and Maastricht Upper Area Control (MUAC) provide air navigation services to the aircraft operators. Due to the high density traffic in the airspace, vectoring or holding manoeuvres are often necessary to maintain proper spacing between aircraft [25]. These come at the cost of additional fuel and noise emissions compared to optimal procedures like CDO. However, before looking into CDO it is important to understand the arrival process of Schiphol first.

2.2 ATM

When an aircrafts want to land at Schiphol it first enters the Dutch airspace via the Flight Information Region (FIR) boundary. The airspace within the FIR is divided and structured into multiple sections. First there is a division between upper airspace (UTA) and lower airspace (CTA) which are controlled by Eurocontrol MUAC and LVNL respectively, as shown in Figure 2.1a [20]. Secondly, the CTA is structured into different sections to accommodate landings at Schiphol Airport, which has the ICAO code: EHAM. The CTA structure can be seen in Figure 2.1b.

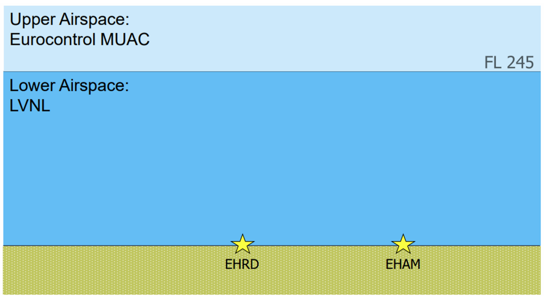

(a) General Airspace Division in Amsterdam FIR.

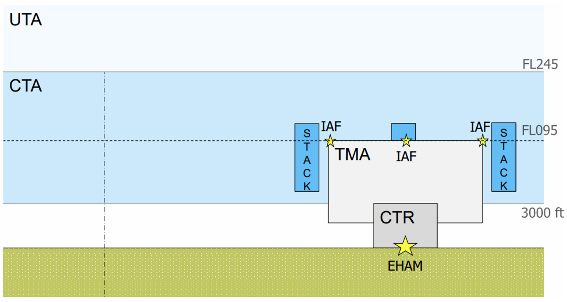

(b) Airspace structure around Schiphol Airport.

Figure 2.1: Dutch airspace structure [20].

Within the CTA, Area Control (ACC) guides the aircraft. For incoming traffic ACC must transfer responsibility of the aircraft within an estimated time of arrival (ETA) of ±2.5 minutes at the Indicated Approach Fix (IAF) to Approach Control (APP). Then APP guides the landing and climbing aircraft to and from the airport in the Terminal Maneuvering Area (TMA). Both ACC and APP are located in the operation room at the main office of LVNL. Stack areas are also allocated to put aircraft in hold if necessary. In Figure 2.2 the arrival routes to the the TMA and the three IAF points are shown [17]. Just before landing, when entering the Control Zone (CTR), Tower (TWR) takes over responsibility. As long as the aircraft is within the CTR and on an active runway TWR guides the aircraft, only after leaving the runway control is transferred to ground control (GND). Of course the reserve is true for outbound flights [17].

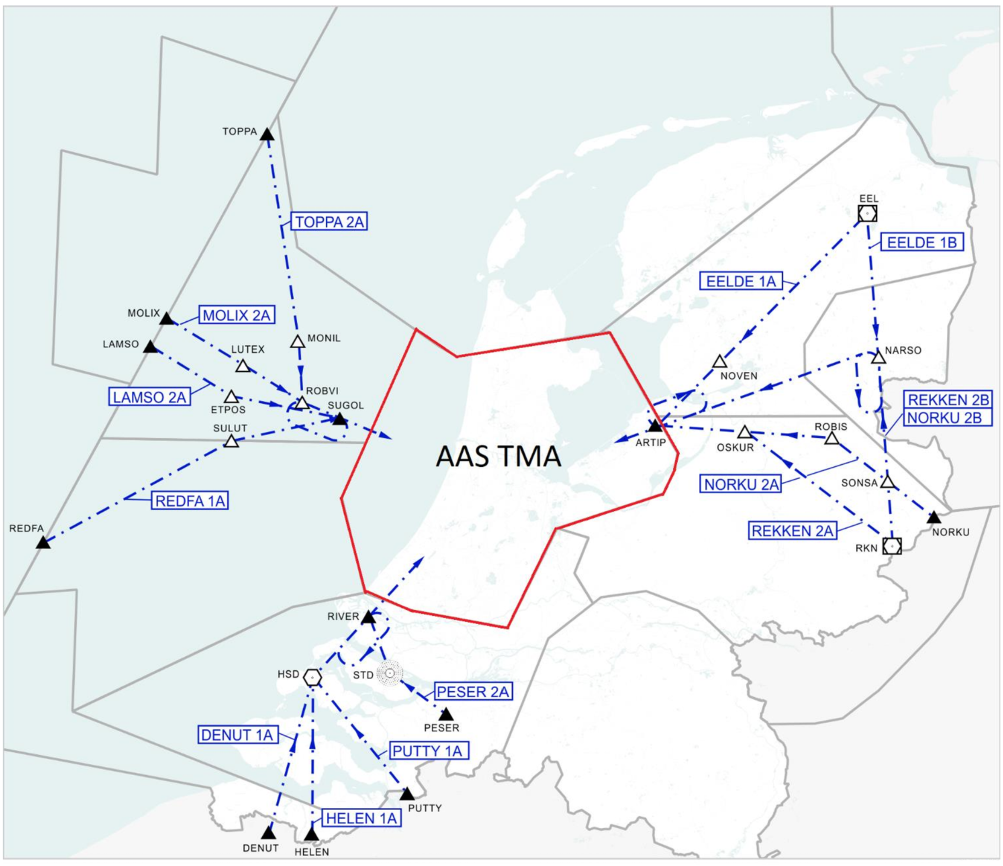

Figure 2.2: Schiphol TMA and IAF points [17].

3 Continuous Descent Operations

This chapter provides information about Continuous Descent Operations. First, in section 3.1 the general definition of CDO is explained. Secondly, two different CDO methods, fixed path angle and idle descents, are covered in section 3.2. Thirdly, section 3.3 analyses the potential fuel benefits of CDO. Finally, the systems allowing CDO to be flown are described in section 3.4.

3.1 Continuous Descent Operations

Continuous Descent Operations, also known as Continuous Descent Approach (CDA), are continuous low thrust trajectory optimized descents. These descents are designed to be more fuel efficient and reduce noise compared to traditional step-down descents. In Figure 3.1 the difference between CDA and conventional step-down approach is illustrated. It should be noted that multiple CDO methods exist, all with different descent profiles, which will be further explained in section 3.2.

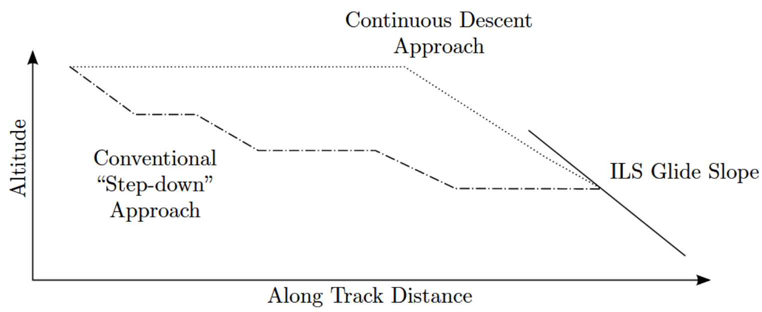

Figure 3.1: CDO versus conventional descent [35].

In general CDO are performed at or near idle thrust settings, flying a uninterrupted descent where level flight segments are avoided [14]. Due to the nature of CDO, the predictability of the aircraft performing the descent decreases compared to a conventional approach. This is caused by CDO being different for each operator, aircraft type, weight and weather conditions [6]. Furthermore the descent is more susceptible to calculation errors since little to no thrust is available for speed or altitude corrections. The aircraft could deploy (additional) spoilers or change it's descent angle to correct for errors, however this would cause the descent to no longer be classified as an continuous descent operation [18].

The decreased predictability has caused problems when trying to implement CDO at airports with busy TMA's or runways. Due to the decreased predictability an increased landing interval of 1.8 to 4.0 minutes has been introduced at Schiphol [40]. This causes a capacity problem during peak hours, hence only night CDO have been introduced so far [18, 33, 40]. In Japan the same problem was encountered, here CDO are only performed at Kansai International, Kagoshima, and Naha. Only during the night and early morning, due to the low predictability and increased complexity for Air Traffic Control (ATC) [19].

Despite this, field tests have showed reductions in fuel consumption [12, 19, 40]. The field test at Schiphol showed a fuel reduction of 25-40% and a significant reduction in noise nuisance [40]. Furthermore, a study from EUROCONTROL showed that only 24% of flights are CDO despite potential average fuel savings of 35kg [15]. Some airports which are less hampered by operational constraints have managed to fly more CDO, of the arrivals at Brussels around 70% are CDO [34]. The results demonstrate that applying CDO can reduce fuel consumption by 21.5 % per flight [41].

3.2 Continuous Descent Methods

CDO is a collective term for different descent methods as mentioned before in section 3.1. Two main descent methods are interesting, the idle descent also known as optimised profile descents (OPD), and the fixed geometric path angle descent (FPA). In general, medium and large sized jet aircraft fly idle descents with the Flight Management System (FMS), further explained in subsection 3.2.1. Smaller jet aircraft often fly FPA instead, which is explained in subsection 3.2.2. As mentioned before the descents differ for each aircraft type, weight, weather conditions and cost index.

3.2.1 Idle Descents

In an idle descent the aircraft initiates descent from top of descent (TOD) after setting the thrust to idle, the minimum thrust required to prevent the engines from stalling. A constant mach is maintained until the crossover altitude, where the aircraft will hold a constant calibrated airspeed (CAS) until the first speed constraint [28]. In the TMA a speed constraint is often implemented and below 10.000 ft the airspeed is constrained to 250KCAS. The descent part before reaching the first speed constraint or ATC intervention is called the performance path. Upon reaching a speed constraint (partial) level segments are introduced in order to decelerate the aircraft. After the TMA and/or altitude speed constrains a final deceleration to final approach speed is required, followed by an increase in thrust to maintain approach speed with flaps engaged [6]. In Figure 3.2 the vertical profile of an idle descent is shown. Segments 1-3 illustrate the TOD and transition from constant Mach to constant CAS. In segments 4-7 the decelerations and level segments are shown. Finally the approach is seen in segments 8 and 9. It should be noted that the length or presence of each segment can change depending on the situation. For example, a TMA with a speed constraint of 250KCAS would mean that segments 4-7 can be done in one step instead. Additionally, deceleration during the descent can be achieved by deploying speed brakes and spoilers. However, according to [28] pilots often avoid this since it increases wear on the aircraft and passenger discomfort.

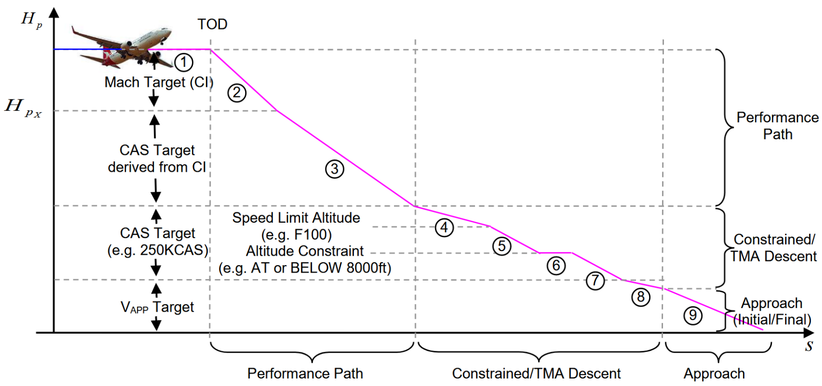

Figure 3.2: Example of a vertical profile of an idle descent.[6]

Although idle descents are the most fuel and noise efficient, implementation into daily operations is difficult. The performance path is very susceptible to aircraft performance and weather conditions, decreasing the predictability [19]. Standard Instrument Arrivals (STARs) have been introduced at some airports to facilitate these descents, however aircraft are often vectored instead by ATC due to capacity and safety requirements [6]. Another descent method, FPA, has been researched in an attempt to solve these implementation issues and will be explained in the next section.

3.2.2 Fixed Path Angle Descent

In a FPA descent the aircraft follows a constant geometric flight path angle. When required thrust or speed brakes are applied in order to maintain this angle. Shallow angles require thrust in order to maintain enough speed and increase flight time. Whilst steeper angle require speed brakes to prevent speed build-up past the flight envelope. Both cause a loss in fuel efficiency compared to idle-descents [19].

However, FPA provides better predictability compared to idle descents whilst still being more fuel efficient than step down descents. The optimum flight path angle for the FPA needs to be calculated for each descent in order to maximize predictability and fuel efficiency [28]. This calculation is still sensitive to aircraft performance and weather conditions [19]. So at the core it is still a matter of balancing predictability versus fuel efficiency for each descent [23].

3.2.3 Descent Equations of Motion

By deriving the equations of motion for descents a basic understanding of the physics can be found. In Figure 3.3 the free body diagram of an aircraft during its descent is shown. The following assumptions were made when deriving the equations of motions and the free body diagrams:

- Spherical and non-rotating Earth.
- The aircraft is rigid and symmetric.
- Thrust angle is parallel to the aerodynamic velocity ($\alpha_T = 0$).
- Symmetric flight.
- γ is negative for descent.
- Steady horizontal winds only depending on altitude.
- Small angles.

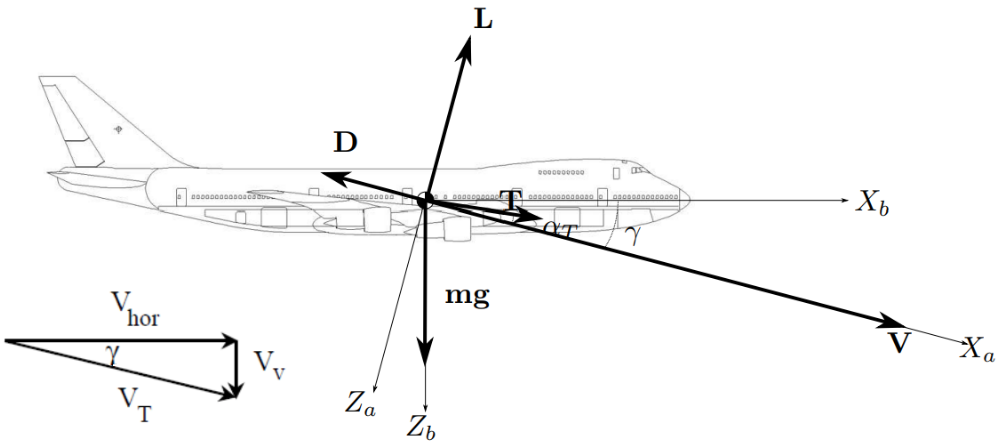

Figure 3.3: Free body diagram of the aircraft[35]

The derivation below is taken from Pradeep and Wei [28] and start with the equations of motion parallel and perpendicular to the aerodynamic flight path shown in Equation 3.1 and Equation 3.2 respectively. First the aerodynamic frame of reference, with flight path angle γ, is considered. Which is later converted to the geometric flight path angle γ_g using Equation 3.10.

$$m\frac{dV_T}{dt} = T - D - mg\sin\gamma - mV_T\frac{dV_{\text{wind}}}{dh}\sin\gamma\cos\gamma \tag{3.1}$$

$$mV_T\frac{d\gamma}{dt} = L - mg\cos\gamma + mV_T\frac{dV_{\text{wind}}}{dh}\sin^2\gamma \tag{3.2}$$

Furthermore Equation 3.1 can be rewritten to Equation 3.3 by assuming small angles.

$$m\frac{dV_T}{dt} = T - D - mg\gamma - mV_T\frac{dV_{\text{wind}}}{dh}\gamma \tag{3.3}$$

The small-angle relation for the aerodynamic flight path angle follows from the air-relative velocity triangle in Figure 3.3. With $V_V = V_T \sin\gamma$ the small-angle approximation gives:

$$\gamma \approx \frac{V_V}{V_T} = \frac{\frac{dh}{dt}}{V_T}. \tag{3.4}$$

Eliminating the time derivative of true airspeed for the altitude derivative in Equation 3.3 gives Equation 3.5. Which can be substituted with γ from Equation 3.4 and rewritten to give Equation 3.6.

$$m\frac{dh}{dt}\frac{dV_T}{dh} = T - D - mg\gamma - mV_T\frac{dV_{\text{wind}}}{dh}\gamma \tag{3.5}$$

$$m\gamma V_T\frac{dV_T}{dh} = T - D - mg\gamma - mV_T\frac{dV_{\text{wind}}}{dh}\gamma \tag{3.6}$$

Equation 3.6 can be rewritten into the following expression for the aerodynamic flight path angle.

$$\gamma = \frac{T - D}{\left(mg + mV_T\frac{dV_{\text{wind}}}{dh} + mV_T\frac{dV_T}{dh}\right)} \tag{3.7}$$

The relation with the geometric flight path angle follows by extending the velocity triangle with an along-track wind component and assuming no vertical wind:

$$\tan\gamma_g = \frac{V_T\sin\gamma}{V_T\cos\gamma \pm V_{\text{wind}}}. \tag{3.8}$$

Applying the small-angle approximation again gives:

$$\gamma_g \approx \frac{V_T\gamma}{V_T \pm V_{\text{wind}}} = \frac{\gamma}{1 \pm \frac{V_{\text{wind}}}{V_T}}. \tag{3.9}$$

Rearranging yields:

$$\gamma \approx \gamma_g\left(1 \pm \frac{V_{\text{wind}}}{V_T}\right). \tag{3.10}$$

The relation between the aerodynamic flight path angle and the geometric flight path angle as shown in Equation 3.10 can be substituted into Equation 3.7. Resulting in the expression for γ_g shown in Equation 3.11.

$$\gamma_g = \frac{T - D}{\left(1 \pm \frac{V_{\text{wind}}}{V_T}\right)\left(mg + mV_T\frac{dV_{\text{wind}}}{dh} + mV_T\frac{dV_T}{dh}\right)} \tag{3.11}$$

Equation 3.11 shows the inherent dependency of an aircraft's descent on wind and atmospheric conditions. Furthermore, rewriting Equation 3.11 to Equation 3.12 shows the thrust required for a continuous descent. It can be seen that negative values for γ will result in lower thrust required, which is why CDO are more fuel efficient and want to avoid any additional segment levels($\gamma_g = 0$) [28]. The fuel and noise benefits of CDO will be further elaborated in section 3.3.

$$T = D + \gamma_g\left(1 \pm \frac{V_{\text{wind}}}{V_T}\right)\left(mg + mV_T\frac{dV_{\text{wind}}}{dh} + mV_T\frac{dV_T}{dh}\right) \tag{3.12}$$

3.3 Fuel Benefits

The fuel and noise benefits of CDO have been extensively researched. These benefits are particularly relevant in high-density terminal airspace such as Schiphol, where operational constraints and environmental impact are critical considerations. It should be noted that most studies cover FPA's and not idle descents. These descents are easier to model and provide better predictability [18]. However, in terms of fuel efficiency idle descents perform similar or better than FPA, depending on aircraft type [18, 28].

One of the most significant contributors to excess fuel burn during descent is the presence of level-off segments. It has been demonstrated that fuel penalties increase with both the length and the altitude of level-offs, with lower altitude segments causing disproportionately higher fuel consumption[16]. Importantly, this relationship is nonlinear, meaning that eliminating level-offs at lower altitudes yields the greatest fuel savings [6]. It is important to note that complete lack of level segments does not immediately constitute an optimal descent. Andreeva-Mori and Uemura [2] showed that minimizing level segments is not necessarily the most fuel efficient descent method. This is because a descent that is to steep, and does not contain any level segments, might need to deploy speed brakes to reduce speed. The energy that is lost during the deployment of speed brakes could have been used to shorten the cruise phase instead by starting the descent earlier.

In Wubben and Busink [40] the impact of idle descents during nighttime operations at Schiphol has been analyzed. From the FMS data of Boeing 747-400 and Boeing 737-300/400 it was concluded that fuel consumption dropped by 25-40%. Furthermore, an inquiry among residents of the surrounding area of the airport also showed a drop in noise nuisance. Reduction in noise emissions is a well known benefit of CDO. This is because of the idle thrust setting and avoidance of speed brakes, reducing noise [30].

Inaad [18] investigated the potential fuel and emission benefits of idle descents implementation at Schiphol. However, FPA's from top of descent (TOD) till the IAF were modeled instead of idle descents to reduce complexity. Average savings of 92kg of fuel could be obtained, however exact savings differed per descent and aircraft type. Potential annual savings of 39 million kg were estimated based on the simulations. Comparisons against previous studies showed that the results were similar to earlier found savings. The paper recommends further research with FMS data and variable flight path angle, as it might increase the fuel benefits. It should be noted that these numbers are not realistically obtainable due to CDO implementation problems. As mentioned earlier, idle descents require more spacing which decreases capacity. Additionally, CDO cause additional flight time [18]. This decrease in capacity might cause delays and holding of other flights which would cause additional fuel burn [10]. Hence the net fuel reduction is smaller than the actual savings of single descents.

3.4 Flight Management Systems & FANS 1/A+

The Flight Management Systems on modern aircraft are capable of executing CDO autonomously. This is done by combining lateral navigation (LNAV), vertical navigation (VNAV) with the flight control system, leaving only flaps and gear deployment to the pilot [28].

Three main VNAV modes can be used during the descent, Vertical Path mode (VPATH), Speed mode (VNAVSPEED) and Required Time of Arrival mode (RTA). During VPATH the FMS follows the given vertical path as accurately as possible. In VNAVSPEED the FMS prioritizes following the given speed schedule. And finally in RTA mode the FMS adapts the descent profile to adhere to the RTA as much as possible [9]. With one or a combination of these modes the FMS calculates the descent profile, incorporating descent parameters such as: altitude constraints, IAF, mass, speed, Cost Index [3]. In general smaller aircraft such as business or regional jets only descend along a FPA using the VPath mode. Larger commercial transport jets are generally designed to fly idle-descents instead by using VPATH and VNAVSPEED, however these are more susceptible to atmospheric conditions due to the idle thrust setting [28].

KLM's long-haul fleet is equipped with the Future Air Navigation System (FANS 1/A+), a data-link communication system that enables digital information exchange between the aircraft and Air Traffic Control. FANS 1/A+ combines two main services, Controller-Pilot Data Link Communications (CPDLC) and Automatic Dependent Surveillance-Contract (ADS-C). CPDLC replaces routine voice messages with standardized digital instructions and clearances. This reduces workload of the pilot and ATC and communication errors. ADS-C automatically transmits the aircraft's position, intent and predicted trajectory. This includes descent-wind data from the FMS to ATC [4, 22]. By uplinking the descent wind data, the FMS can calculate its descent more accurately although the amount of data that can be uploaded is limited. By improving the FMS performance and sharing the FMS intent with ATC, FANS 1/A improves predictability of idle thrust descents and its operations [12].

4 Idle-Descents Predictability

The following chapter goes in-depth into the predictability of idle descents. First, section 4.1 highlights the importance of predictability. In section 4.2 the impact of control methods on the predictability is explained. This is followed by an extensive analysis of the influencing variables and impacts in section 4.3.

4.1 Importance of Predictability

Now that the benefits and workings of idle descents have been covered, the impact of trajectory uncertainties are considered. In section 3.1 the additional spacing required and resulting implementation issues were already mentioned. Studies have shown that reducing the unpredictability can help with implementing CDO. An analysis of the impact of the CDO's prediction accuracy has been done by Raghunandan [29]. In this study simulations with different prediction accuracies were performed. Results showed a significant improvement in amount of CDO flown when the prediction accuracy was improved. It should be noted that the study only considered non-idle descents and investigated the prediction accuracy of ATC, not the general variability of FMS prediction error. However, the results of the study are still promising for the impact of improving idle descent predictability. As a more accurate ATC Trajectory Predictor (TP) is arguably more important than the FMS TP when looking at the airport capacity impact.

Apart from allowing CDO to be flown, reducing trajectory uncertainties can also improve the descent efficiency itself. Fricke, Seiß, and Herrmann [16] showed that aircraft type, mass and meteorological parameters are vital for the optimal descent profile. Hence, understanding the influence of uncertainties in these parameters is important as it can impact descent performance.

4.2 Control Methods

The control method of an aircraft during its descent dictates how uncertainties impact the descent. The earlier derived EOM of continuous descents in subsection 3.2.3 by [28] show the inherent susceptibility of an idle descent to the aircraft performance, descent speed profile and atmospheric conditions. Idle descents are flown at set idle throttle and vertical or speed profile. According to Equation 3.11 any deviations in drag (governed by atmospheric conditions) and wind result in a change in γ, when flying a speed managed descent. This is achieved by using elevator control to manage the speed, in turn altering γ. In Figure 4.1 the possible accumulation effect of these errors in case of a speed managed descent is shown, and the elimination of them during step-down descents.

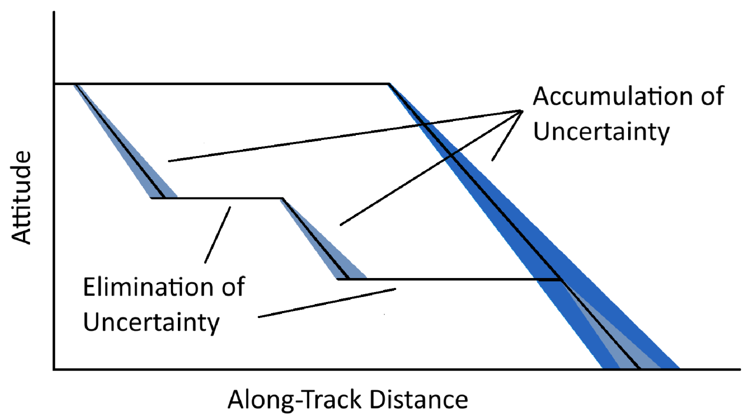

Figure 4.1: Accumulation of uncertainty errors during continuous and step-down descents, adapted from Pradeep and Wei [28]

This deviation in γ can be prevented, however this would result in thrust/speed brake usage or speed deviations. So it is important to note that depending on the control method, errors in descent calculations, predictions or execution have a different impact on the predictability. The control logic of the aircraft can be adapted to strike a preferred balance between: altitude, speed, and energy efficiency [23]. For example, the vertical profile uncertainty shown in Figure 4.1 can be reduced by flying a path managed descent instead. This adversely affects the speed and temporal predictability of the descent but provides a consistent descent path and is the most economical descent strategy [9].

In Dalmau and Prats [13] the feasible time window at the IAF was investigated by simulating a new guidance control law. It simulated idle descents where only elevator control was allowed to alter the time window. Although, it was possible to increase the feasible time window and thus the probability of executing a full idle descent. It was concluded that this came at the costs of additional fuel consumption. Turgut, Usanmaz, and Rosen [39] showed that this penalty can be minimized by designing the descent accordingly. However, some optimal descent strategies could cause additional pilot workload and flaps wear [35].

Hence completely eliminating all errors whilst maintaining an optimal descent is an almost impossible task. Speed or γ perturbations will always remain due to aircraft modeling, weather forecast or control limits. However, an in-depth look into what causes these errors can aid us in quantifying and reducing them.

4.3 Influencing Variables and Impacts

Multiple variables influence the predictability of idle-descents. As discussed in the previous section, the impact of these factors is depending on the descent method. Additionally, other parameters such as aircraft mass, type or performance can also influence the impact these variables have [37]. Finally, the perspective from which the predictability is analyzed is also important when considering which factors are impact full. For example, a ground TP continuously updates descent predictions with new weather and surveillance data, while an FMS uses closed-loop guidance to minimize tracking error and recomputes its trajectory as conditions change. Hence, it is vital to carefully consider the methods of a study before drawing any conclusions from it's results.

4.3.1 Equations of Motion

From the EOM derived in subsection 3.2.3 a basic understanding of the influencing variables can already be gained. The flight path angle of the idle descent will decrease (steeper descent) with an: increase in weight, increase in drag, decrease in speed, increase in tailwind or positive wind gradient (increasing tailwind with altitude). If an aircraft descends through unconstrained airspace the idle descent path is only limited by the γ boundaries. Since beyond certain γ the aircraft's velocity would exceed the operational envelope. When imposing airspace and CI constraints like distances, flight time or fuel efficiency on the idle descent the main control variable is the TOD location. The distance from TOD till end of descent fix decides how much energy the aircraft has during the descent, which is used to fly certain γ's and velocities. Figure 4.2a for examples shows the shift in TOD required when encountering 10kts headwind instead of tailwind, when computing the idle descent path from Equation 3.11. Furthermore, the effect of the speed schedule on the descent path is shown in Figure 4.2b. As mentioned before in subsection 3.2.1 speed brakes and additional thrust can be used for more acceleration/deceleration during the descent, shortening the transition segment. However shifting the TOD is still the preferred solution as this would provide the most fuel efficient descent.

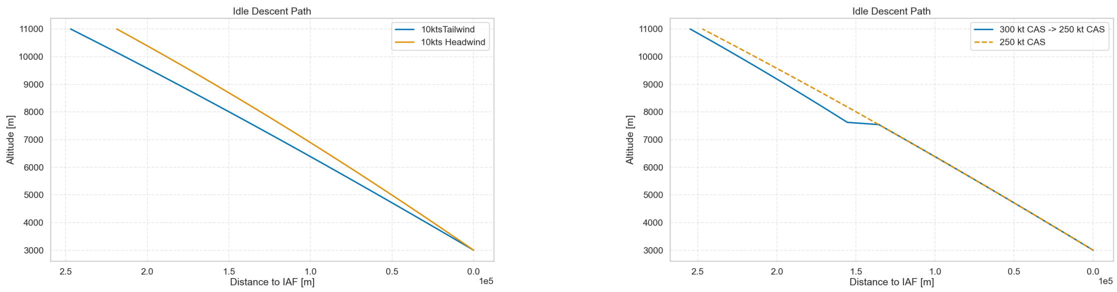

(a) Idle descent path with 10 kts headwind and tailwind. **(b)** Idle descent path with constant and variable speed schedule.

Figure 4.2: Idle descent reference paths constructed from EOM's under different wind and speed schedule assumptions.

Any deviations in flight path angle will result in a different vertical path, speed schedule, or flight time. As mentioned before the dependency on drag and wind show the vital role of the atmospheric and weather conditions on the unpredictability of idle descents. Furthermore, the FMS uses wind predictions to calculate the descent. However, when these predictions do not match the actual wind conditions the aircraft defers from the calculated path. This can lead to additional steady level flight segments or speed brake deflections [3].

4.3.2 General FMS Inputs

In Bronsvoort et al. [8] it was demonstrated that with improved input data for ground trajectory predictors (TP), uncertainties can be reduced. The study used data from FANS equipped aircraft landing at Melbourne. Additional mass inputs from the FMS slightly improved the vertical profile and greatly improved the TOD prediction. Including the down linked profile of the FMS further reduced the altitude profile errors, although little improvements of the temporal accuracy were observed. The temporal accuracy did saw great improvements when incorporating the descent schedule of the FMS into the TP. With this the TP even managed to attain a better temporal accuracy than that of the FMS down-linked trajectory. This was due to the higher resolution weather forecast that was available for the ground TP. The additional accuracy that was obtained by including the descent schedule is only relevant for improving the predictability of ground TP's. However, the additional temporal accuracy that resulted from using higher weather resolution data is an important finding that highlights the importance of accurate weather data when modeling idle descents.

4.3.3 Guidance Laws

Ledesma and Navarro [23] presents a FMS guidance law to maximize predictability. It mentions how wind uncertainty will affect aircraft differently depending on type, conditions and guidance law. It tries to minimize the influence of wind, mass and control uncertainties by improving the guidance law. Simulations of B737-700 were performed starting at 10.000ft and ending at 2000ft. Errors in the wind gradient, control law and weight were introduced and their impact was analyzed. Result showed little time deviation due to deviations in wind gradient or weight. However large time deviations due to inaccuracies in the γ execution were found. A sustained error of +- 0.05 degrees would cause +-4 seconds of flight time, extrapolating this to a descent from TOD at around 30.000ft would mean +- 12 seconds. Tailwinds magnify this error, likely due to the longer track distance it causes.

4.3.4 Weather Uncertainties

The FMS and TP's make use of weather forecast to predict the flight trajectory of aircraft. However, these forecast contain inaccuracies impacting the predictability of flights. Magaña [26] mentions average wind speed errors of $3.5m/s$ and temperature deviations of $2K$. When enough data measurements are available for a specific area and time, nowcasts can reduce these errors to approximately $2.5m/s$ and $1K$.

Uncertainties in wind speeds are especially important since it directly impacts ground velocity, an important parameter for ATC [26, 11]. This can clearly be seen when analyzing the along track difference of two aircraft who are following the same trajectory. In [24] this difference is expressed using Equation 4.1.

$$Total\ Along\ Track\ Difference = \sum_{i=1}^{n}[(V_{ground\_ref} - V_{ground\_test}) * \Delta t]_i \tag{4.1}$$

Here V_{ground_ref} and V_{ground_test} are the ground speeds for the reference and test trajectories respectively, for example the FMS predicted trajectory and the actually flown trajectory. Substituting V_{ground} for $V_{TAS} + V_{Wind}$ yields Equation 4.2.

$$Total\ Along\ Track\ Difference = \sum_{i=1}^{n}[((V_{TAS\_ref} + V_{Wind\_ref}) - (V_{TAS\_test} + V_{Wind\_test})) * \Delta t]_i \tag{4.2}$$

When the intended speed schedule ($\sum_{i=1}^{n}[V_{TAS}]_i$) is known the reference and test trajectory airspeeds are equal. The following expression can be derived which shows the impact of the wind speeds on the along track difference in Equation 4.3.

$$Total\ Along\ Track\ Difference \approx \sum_{i=1}^{n}[(V_{Wind\_ref} - V_{Wind\_test}) * \Delta t]_i \tag{4.3}$$

Magaña [26] also found a clear correlation between the standard deviation of the along track wind speed and the ground speed, as shown in Figure 4.3. This demonstrates the dependency of trajectory predictability on the weather conditions.

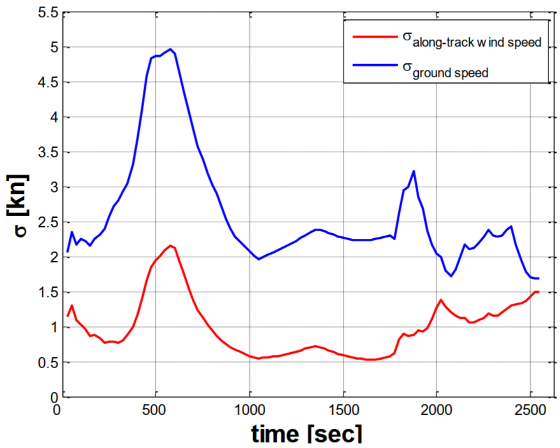

Figure 4.3: Along-Track Wind speed and Ground Speed Standard Deviations [26]

.

4.3.5 Wind Uplink

In Coppenbarger and Mead [12], operational trials for idle descents were done at San Francisco, called the Oceanic Tailored Arrivals (OTA) trials. During the OTA trials a special procedure for a Boeing-777 was used to analyze it's effect on enabling continuous descents in constrained airspace. From data of flights flown over 40 days the fuel benefits and trajectory performance were analyzed. Results not only showed a reduction in fuel usage, but also a clear reduction in temporal prediction error after uplinking wind data. This can be seen in Figure 4.4, the EDA descent-speed uplink effects can be ignored since these were used to synchronize the FMS and ground TP speed schedules.

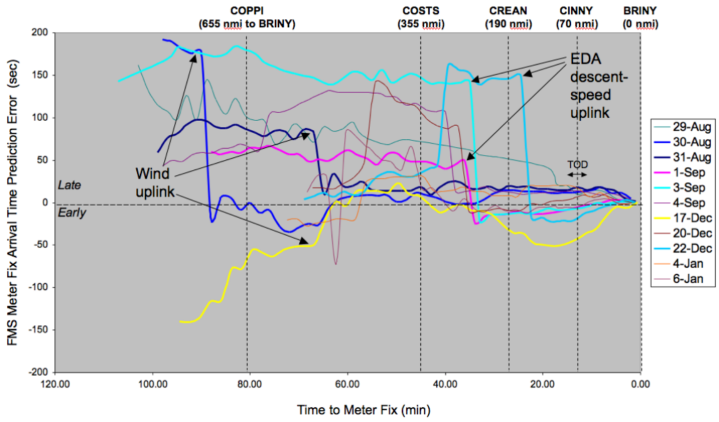

Figure 4.4: Effect of wind uplink on FMS arrival-time prediction [12]

A few years after the start of the OTA trials a second study investigated the FMS execution of idle descents using an extended version of the original dataset, still only from a single B777 [36]. The author of this study had performed a similar analysis using a B737 flight simulator a few year earlier in Stell [37]. The intended performance was compared to the actual performance of all suitable descents, comparing the lateral and vertical tracks, airspeeds and IAF crossing times. It was found that the airspeed is usually withing 0.01 of the target Mach and within 10KCAS of the target CAS, which would result in a temporal error between TOD and IAF of about 20-35 seconds. Further analysis of the actual and FMS predicted IAF crossing times showed an even larger error of about 50 seconds. Hence, the paper concludes that about half of this error can be attributed to execution errors of the speed schedule, and the other half to other major sources like descent wind forecast errors. It also stated that the former part of the error can likely not be reduced, which could be explained by limitations of the FMS. This is also supported by Pradeep and Wei [28], which states that the FMS performance model might not be accurate enough to predict actual aircraft responses in idle thrust to atmospheric and weather conditions.

During tailored arrival trials in Melbourne it was attempted to improve the descent wind inputs and reduce speed schedule deviations [7]. This was done by computing a tailored descend wind forecast for each descent. Since uplink data is limited, only wind data at a few flight levels can be uploaded. The FMS then interpolates the data to create a complete descent wind profile. In Figure 4.5 the possible resulting deviations in the wind profiles are shown. Additionally, it was stated that prediction errors in the base forecast data will also result in errors during the descent. Finally, deviations between the planned and flown trajectory also cause errors in the wind profile.

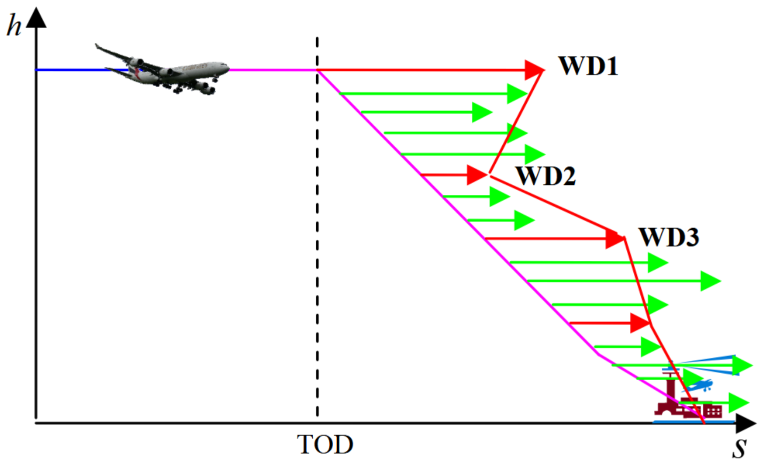

Figure 4.5: Interpolated wind profile versus actual wind profile [7].

Bronsvoort et al. [7] showed that any wind profile errors would result in groundspeed and geometric path errors. This is due to the wind profile affecting the predicted TAS, flight path and drift angles, and tail or headwinds. This can be seen in Equation 4.4, the first two components indicate the indirect effect of a change in descent path due to prediction errors and the third component the direct effect of prediction error. Furthermore, the paper converts the groundspeed error to a temporal error using Equation 4.5.

$$\Delta V_g = (V_{\text{TAS}} + \Delta V_{\text{TAS}}) \cos(\gamma_{\text{TAS}} + \Delta\gamma_{\text{TAS}}) \cos(\chi_{\text{dr}} + \Delta\chi_{\text{dr}}) - V_{\text{TAS}} \cos\gamma_{\text{TAS}} \cos\chi_{\text{dr}} + \Delta w_{tl} \tag{4.4}$$

$$\Delta T = \int \frac{1}{\Delta V_g(s)}\, ds \tag{4.5}$$

The study aimed to reduce the identified components of the wind profile prediction: base forecast prediction error, forecast grid cell selection error, and interpolation error. This was done by first applying the planned trajectory to a higher resolution weather forecast grid and re-computing the trajectory according to predicted conditions. Afterwards, the uplinked wind data was tailored to minimize the error between the interpolated weather profile and the base weather prediction profile. After designing the Tailored Descent Winds Tool its performance and impact was analyzed during the flight trials with arrivals into Melbourne.

Although the study managed to reduce wind prediction errors from planned trajectory deviations and interpolation, the analysis on its impact was limited. The new higher resolution weather forecast proved to be less accurate than the original forecast data. Furthermore, only data of two A345 flights were gathered, both flying the same route, one with and one without the tailored descent winds. The aircraft flew their descents with the VPATH mode, meaning that wind profile errors would mainly result in speed deviations. All flights showed large deviations between the target and actual speed profiles, uncorrelated to the prediction error in descent winds. This obscured any improvements of descent efficiency, however possible temporal accuracy improvements were observed.

More recent analysis on the impact of wind uplink to the FMS has also been done. Jones et al. [21] simulates the effect of different wind uplinks on the RTA performance of the FMS. In the study B757-200 descending according to a RTA tolerance of six seconds and a CI of 50 were simulated. It is difficult to infer how close these descents parameters resemble a fully idle-descent. The effects of three uplink scenarios with different resolutions were analysed. Firstly no forecast data uplink was considered, giving base values. Afterwards wind uplink data optimized for magnitude, headwind or equidistant altitudes were tested at four and nine levels. Uplinking four forecast levels significantly improved the RTA performance compared to no wind uplink, going from about 53.4s mean RTA error to under 4s. Further improvements when uplinking nine levels were found, although these are of much smaller magnitude (0.5s). Optimizing the forecast for magnitude proved most optimal, and a large impact on RTA performance by procedural speed constraints was found.

Simulation results from Tom G. Reynolds [38] further support these findings. The study considered three combinations of aircraft and FMS's: B737-700 with full flight phase RTA, B757-200 with cruise only RTA or a prototype full flight phase RTA. Monte Carlo simulations with changing permutations for each descent were performed. It concluded that wind forecast errors in magnitude, location and variability have a considerable impact on RTA performance. Furthermore, it was found that FMS RTA capability also has a large impact on the RTA performance. Ahmad, Barmore, and Swieringa [1] also found an slight improvement of descent forecast when uplinking more altitude levels. However the simulation model used partially corrected wind errors which obscured the impact on speed deviations. Additionally, it stated that the wind profile used was quite smooth and similar for each route, further limiting wind errors.

Ostertag [27] conducted a case study that investigated the impact of the wind uplinks on fuel efficiency during descent. LH Cargo upgraded its weather forecast data after pilot input expressed potential in improved wind data. The study investigated the impact of linking this improved data set with the FMS via the Avtech tool Aventus NowCast. This tool communicates directly via data link, similarly to the systems described in section 3.4. The trial gathered ten months of data from twelve MD11F aircraft.

It showed an average reduction of about 50% in wind error predictions during cruise and descent. Furthermore the reduced errors proved a lot less volatile. In order to motivate investment in the new system, fuel savings from TOD till FL100 were calculated using performance tables. Average potential fuel savings of 26kg per flight during the descent were found, although a more conservative estimate of 17kg was used for the business case. The conservative estimate took into account that due to operating constraints, the system would not be used for every descent. Additionally, daily performance analysis showed larger fuel savings during unstable weather conditions. After the succesfull trial, LH Cargo installed the Aventus system on all the MD11F and Boeing 777F aircraft.

5 Research Foundations

In this chapter the research foundations of this study are presented. In section 5.1 the knowledge gaps, derived from the previous chapters, are highlighted. Based on this the research objective is formed in section 5.2. Followed by the research questions and impact to support this objective in section 5.3 and section 5.4.

5.1 Identified Knowledge Gaps

From section 3.3 it can be concluded that idle descents offer considerable benefits in terms of fuel efficiency, emissions, and noise reduction. However implementation of idle descent at high traffic airports is difficult due to additional uncertainties in trajectory predictions. Previously performed flight trials, such as the OTA trials [12] and the tailored arrival trials in Melbourne [7], have shown that a large part of the trajectory variability is due to wind prediction errors. Although these studies provide valuable insight into descent behavior, several key knowledge gaps persist.

Analytical analysis of an idle descent in subsection 3.2.3 showed the inherent sensitivity of the descent to drag, atmospheric- and wind condition variations. Furthermore, section 4.2 highlights that the control method of an idle descent determines how uncertainties due to these disturbances propagate through the trajectory. Ledesma and Navarro [23] even showed how small deviations in γ affect the temporal accuracy of the descent. However these results were based on simulations requiring assumptions and simplified conditions. Empirical quantification of these uncertainties, from experimental descent data, is still limited.

Studies that have gathered experimental data, during normal operations or flight trials, have demonstrated the importance of meteorological input data. The OTA trials demonstrated that uplinking descent winds can substantially reduce RTA error for idle desents. However these results were based on trials with a single Boeing-777. Further analysis of extended data from this trial showed that approximately half of the RTA error is due to descent wind prediction errors, with the remainder attributed to FMS execution limits and speed constraints. Other studies showed improved wind profile predictions when optimally fitting or adding uplink levels [7, 21, 38]. Empirical work of Bronsvoort et al. [7] did not manage to quantify the impact of wind prediction error on RTA performance. The other studies did find improved RTA performance, however these results were based on simulations and not experimental flights. Empirical work by Ostertag [27] did show promising fuel savings due to improved wind predictions. However, the study did not consider its impact on temporal accuracy. Yet the business case did manage to convince LH Cargo to invest in the Aventus NowCast system. Furthermore, KLM has also invested in meteo uplink, recently even extending it to their 737's with Airline Operation Control(AOC) Datalink.

So while prior research has demonstrated the sensitivity of idle thrust descents, only limited data-driven quantification of their relative contributions under real airline operations exists. Moreover, recent experimental analysis do not cover modern aircraft types or are performed at Schiphol airport. This research aims to address these gaps by using high-fidelity KLM Flight Data Recorder (FDR) and FMS wind uplink data to statistically relate wind-prediction errors to descent efficiency and temporal accuracy across multiple aircraft types and descent conditions.

5.2 Research Objective

Now that a knowledge gap has been identified in the literature, the research objective of this study can be formulated. The research objective of this thesis is as follows:

Research Objective

The objective of this research is to quantify and manage the sources of uncertainty affecting idle thrust continuous descents at Schiphol. This includes analyzing how errors in uplinked descent winds influence the efficiency and temporal accuracy of these descents, and identifying additional factors that contribute to trajectory variability.

The research objective consists of multiple components. First identification and quantification of factors that contribute to uncertainties of idle thrust must be performed. Secondly, the precise effect of these factors on descent efficiency and temporal accuracy must be calculated. Finally, mitigation strategies to reduce the impact of such errors will have to be formed.

5.3 Research Questions

To help with reaching the research objective, research questions (RQ) are formulated. First the main research question is derived from the research objective. The main research question already lays a focus on wind uplink, however it is still quite broad.

Main Research Question

How do inaccuracies in FMS descent winds and other operational factors influence idle descent efficiency and temporal accuracy, and how can these uncertainties be managed?

In order to provide more concrete research question four additional sub question were formulated from the main research question. This was done to give more precise goals during the thesis duration. RQ:1 and RQ:2 focuses on analyzing the impact of wind prediction errors. RQ:3 specifies the analysis of other factors and RQ:4 looks into the mitigation efforts.

Sub-Question 1

How do wind prediction errors in the FMS affect descent efficiency in terms of speed deviations and fuel burn?

Sub-Question 2

How do wind prediction errors in the FMS influence along-track time accuracy and arrival-time predictability during idle thrust continuous descents?

Sub-Question 3

Which other operational or environmental factors (e.g., aircraft type, mass variation, or atmospheric conditions) significantly contribute to idle descent trajectory uncertainty?

Sub-Question 4

How can the identified uncertainties be managed or mitigated through wind uplink, trajectory updates, or procedural adaptations?

5.4 Research Impact

The findings of this research are expected to advance both the scientific understanding and operational management of Continuous Descent Operations at major hub airports. From an academic perspective, the study contributes a data-driven quantification of descent trajectory uncertainty, extending previous simulation-based and experimental work. By empirically linking FMS wind uplink data to observed speed and time deviations, the results will provide new insight into how information uncertainty propagates through the descent guidance process. Furthermore, possible fuel benefits can be further defined. This will help refine existing trajectory-prediction models and performance-based navigation frameworks used in both research and system development.

From an operational standpoint, the outcomes will support ongoing efforts by the Knowledge Development Centre (KDC) and the aviation industry to enable predictable, low-noise, and fuel-efficient idle descents during daytime operations at Schiphol. The results of the study can possibly motivate investments into improved FMS wind uplink and modelling systems. Ultimately, the work aims to bridge the gap between environmental efficiency and operational predictability, enabling wider adoption of continuous idle thrust descents.

6 Research Plan

This chapter contains the research plan of the study. First, the methodology is described in section 6.1. Secondly, the hypothesis is presented in section 6.2. Finally, section 6.3 visualizes the planning according to a Gantt Chart and flowchart.

6.1 Methodology

In order to fulfill the research objective and answer the research questions the methodology of the study has been outlined. The work has been divided into multiple work packages (WP), with each package building upon the previous steps. First data acquisition and preprocessing is performed, followed by a quantitative analysis of the data. Finally, mitigation strategies and possible extensions such as flight trials or TP enhancement are added.

6.1.1 WP 1: Data Acquisition and Preparation

The first work package focuses on obtaining and organizing the datasets required for the study. KLM will provide high fidelity FDR data and wind uplink data from CDO of multiple aircraft types. The FDR data contains parameters such as altitude, Mach, CAS, lat, lon, thrust setting, fuel use, flap settings, spoiler deployment at five second intervals.

The FDR data will be anonymized so information such as dates and flight numbers are not available. However a few unanomymized flights can possibly be made available. Hence, selecting these flights can best be done after initial research on the original dataset has progressed. After collection of the data it will need to be cleaned and parsed before further analysis.

6.1.2 WP 2: Idle Descent Identification

Due to the size of the data set idle descents identification will have to be automated using python. Idle descents could be detected with a combination of [6]:

- Low thrust setting
- No level-off segments
- No abrupt speed or altitude changes
- Minimal speed brake or spoiler deployment

Note that possible speed brake or spoiler deployment can still be a part of the idle descent, when an aircraft exceeds speeds constraints during it's automated descent. The output of this work package will be a filtered dataset consisting of suitable idle descents for further analysis.

6.1.3 WP 3: Wind Uplink Analysis

After the filtered dataset has been prepared, detailed analysis into FMS descent winds inaccuracies and their impact can start. The root mean squared error (RMS) of the wind prediction and target speed can be used to quantify wind uplink inaccuracies and resulting speed deviations, as shown in Equation 6.1 and Equation 6.2 [7]. Here $\hat{\mathbf{w}}_{FCST}(h_i)$ and $\bar{\mathbf{w}}_{AC}(h_i)$ are the wind forecast and actual wind at specific altitude h_i. Actual wind speeds will have to be derived from ground velocity and true airspeed. In Equation 6.2, $V_{CAS_{\mathrm{TARGET}}}(H_p)$ and $V_{CAS}(H_p)$ are the target CAS and actual CAS at specific altitude H_P.

$$RMS_{\mathbf{w}}\left(\hat{\mathbf{w}}_{FCST}\right) \equiv \sqrt{E\left[\sum_{i=1}^{n} \|\hat{\mathbf{w}}_{FCST}(h_i) - \bar{\mathbf{w}}_{AC}(h_i)\|^2\right]} \tag{6.1}$$

$$RMS_V(\Delta V_{CAS}) = \sqrt{E\left[\left(V_{CAS_{\mathrm{TARGET}}}(H_p) - V_{CAS}(H_p)\right)^2\right]} \tag{6.2}$$

Furthermore, the effect on fuel efficiency will be analyzed. For this the fuel use during the descent will have to be compared to the wind uplink inaccuracies. Finally, speed errors need to be converted to temporal accuracy to properly quantify the possible effects on airport capacity.

6.1.4 WP 4: Analysis of Additional Factors

Now that the initial relation between wind uplink inaccuracies and idle descent performance have been found a more detailed analysis on additional factors can be performed. The effects of e.g., aircraft types, mass, altitude and atmospheric conditions will be studied. This will involve comparing descent performance across different aircraft types and weights, and examining how varying atmospheric conditions correlate with deviations. Resulting in a better and broader understanding of the uncertainties of idle descents.

6.1.5 WP 5: Mitigation Strategies

With a complete understanding of the idle descent trajectory uncertainties, possible mitigation strategies can be designed. Possible strategies will have to be discovered and tested. This could involve further analyzing the effect of wind uplink inaccuracies through flight trials. After simulating the effects of wind inaccuracies in the FMS in BlueSky or properly defining the relation between wind uplink inaccuracies and flight performance. Explicitly uplinking wrong wind data to descending aircraft or facilitating full idle descents, can validate these findings. During this validation, more accurate TP's can potentially be designed and further tested. Furthermore, improved wind uplinks at Schiphol can also be tested during such trials. These improved uplinks could make use of tailored uplinks or higher resolution forecast as tried before by Bronsvoort et al. [7].

6.2 Hypothesis

Based on the research presented in this study, and the proposed methodology, the following hypotheses are formulated. Wind prediction errors are expected to be a primary driver of speed and timing deviations during idle descents. FMS accuracy and other parameters will also contribute to these errors, preventing complete eliminations of speed and time deviations. Furthermore, wind prediction errors will lead to increased fuel consumption and other parameters will modulate the sensitivity of descent performance to wind uplink errors. Finally, improving wind uplink quality or understanding the effect of wind inaccuracies can support the implementation of idle descents into the operations of high density airspace such as Schiphol Airport.

6.3 Planning

In Figure 6.2 the thesis outline is displayed in a Gantt Chart. The timeline takes into account an 80% workload and holidays according to the academic calendar. In Figure 6.1 the work flow of the work packages is shown. Two vital work packages have been identified, WP 1 and WP 2. Progress of the study is severely limited until the data from KLM has been received and data preperation can start. However, CDO data for another thesis can be used whilst waiting for the KLM data. Furthermore, the analysis of idle descents can only be performed after idle descents are correctly identified and gathered in a new dataset. A final important note is on WP 5, if flight trials are to be done work on this should start as soon as possible. This is due to the fact that this is again highly dependent on collaboration with KLM.

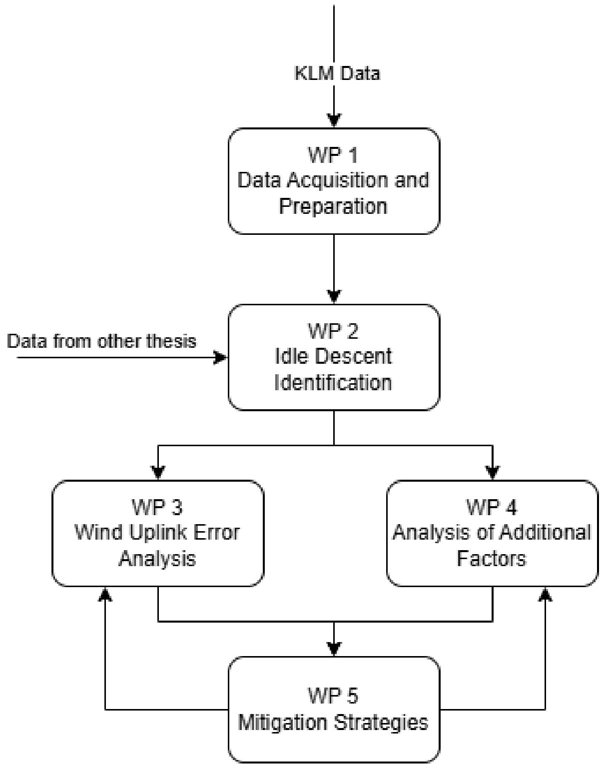

Figure 6.1: Flow chart of the work packages.

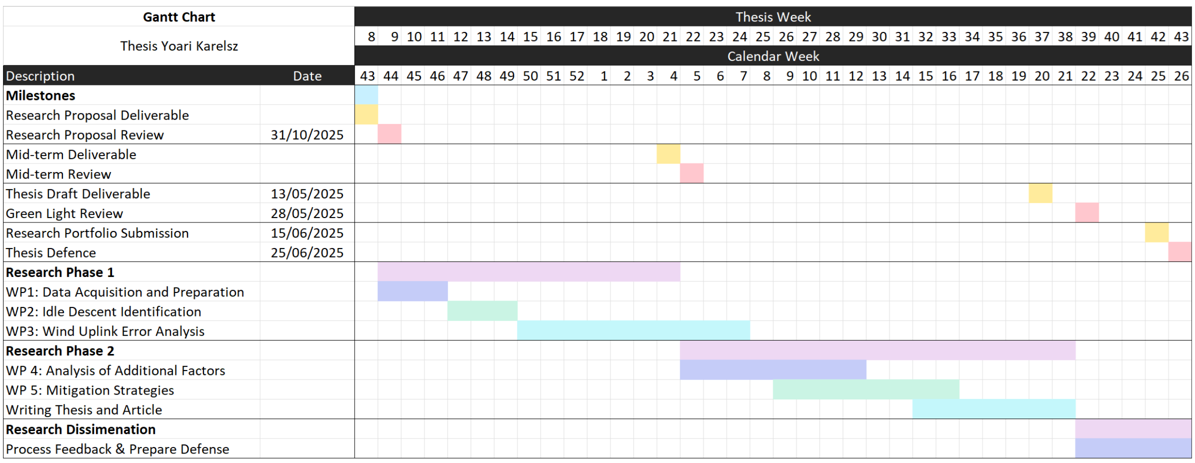

Figure 6.2: Gantt Chart

References

[1] Nashat Ahmad, Bryan Barmore, and Kurt Swieringa. "Wind Information Uplink to Aircraft Performing Interval Management Operations". In: 15th AIAA Aviation Technology, Integration, and Operations Conference. Dallas, Texas, USA: American Institute of Aeronautics and Astronautics (AIAA), 2015. DOI: 10.2514/6.2015-3398. URL: https://arc.aiaa.org/doi/10.2514/6.2015-3398 (visited on 10/20/2025).

[2] Adriana Andreeva-Mori and Tsuneharu Uemura. "Efficiency Analysis of Speed Managed Descent in the Presence of Wind Prediction Error". en. In: *TRANSACTIONS OF THE JAPAN SOCIETY FOR AERONAUTICAL AND SPACE SCIENCES* 61.1 (2018), pp. 1–11. ISSN: 0549-3811, 2189-4205. DOI: 10.2322/tjsass.61.1. URL: https://www.jstage.jst.go.jp/article/tjsass/61/1/61_T-16-48/_article (visited on 09/24/2025).

[3] Adriana Andreeva-Mori and Tsuneharu Uemura. "Optimal Top of Descent Analysis in Respect to Wind Prediction Errors and Guidance Strategies". en. In: *TRANSACTIONS OF THE JAPAN SOCIETY FOR AERONAUTICAL AND SPACE SCIENCES, AEROSPACE TECHNOLOGY JAPAN* 15.APISAT-2016 (2017), a45–a51. ISSN: 1884-0485. DOI: 10.2322/tastj.15.a45. URL: https://www.jstage.jst.go.jp/article/tastj/15/APISAT-2016/15_TJSAS-D-17-00011/_article (visited on 09/24/2025).

[4] Universal Avionics. *Understanding Data Comm Systems with Domestic and Oceanic FANS 1/A+ and ATN B1 Services*. 2020. URL: https://www.oregonflightschool.com/uploads/4/6/3/3/46333289/fans-cpdlc-ads-c-oregon-flight-school.pdf.

[5] Hendrik van Beuningen. *KLM Boeing 737-8K2*. URL: https://nl.pinterest.com/pin/374784000260911411/ (visited on 10/06/2026).

[6] Jesper Bronsvoort, Trang Huynh, and Gabriele Enea. "An Operator-Focussed Metric for Measuring Predictability and Efficiency of Descent Operations". en. In: *16th AIAA Aviation Technology, Integration, and Operations Conference*. Washington, D.C.: American Institute of Aeronautics and Astronautics, June 2016. ISBN: 978-1-62410-440-4. DOI: 10.2514/6.2016-4219. URL: https://arc.aiaa.org/doi/10.2514/6.2016-4219 (visited on 09/24/2025).

[7] Jesper Bronsvoort et al. "Enhanced Descent Wind Forecast for Aircraft". In: Ninth USA/Europe Air Traffic Management Research and Development Seminar (ATM2011). Berlin, Germany, June 2011, pp. 1–10.

[8] Jesper Bronsvoort et al. "Impact of Data-Link on Ground-Based Trajectory Prediction Accuracy for Continuous Descent Arrivals". en. In: *AIAA Modeling and Simulation Technologies (MST) Conference*. Boston, MA: American Institute of Aeronautics and Astronautics, Aug. 2013. DOI: 10.2514/6.2013-5068. URL: https://arc.aiaa.org/doi/10.2514/6.2013-5068 (visited on 09/24/2025).

[9] Jesper Bronsvoort et al. "Understanding time-drift for different aircraft descent guidance strategies". In: ATACCS'2012. London, UK: ATACCS, 2012. ISBN: 978-2-917490-20-4.

[10] Yi Cao, Daniel DeLaurentis, and Dengfeng Sun. "Benefit and Trade-Off Analysis of Continuous Descent Approach in Normal Traffic Conditions". en. In: *Transportation Research Record: Journal of the Transportation Research Board* 2325.1 (Jan. 2013), pp. 22–33. ISSN: 0361-1981, 2169-4052. DOI: 10.3141/2325-03. URL: https://journals.sagepub.com/doi/10.3141/2325-03 (visited on 10/02/2025).

[11] Georgios Chaloulos and John Lygeros. "Effect of Wind Correlation on Aircraft Conflict Probability". en. In: *Journal of Guidance, Control, and Dynamics* 30.6 (Nov. 2007), pp. 1742–1752. ISSN: 0731-5090, 1533-3884. DOI: 10.2514/1.28858. URL: https://arc.aiaa.org/doi/10.2514/1.28858 (visited on 11/18/2025).

[12] Richard A Coppenbarger and Rob W Mead. "Field Evaluation of the Tailored Arrivals Concept for Datalink-Enabled Continuous Descent Approach". In: 7th AIAA Aviation Technology, Integration and Operations Conference (ATIO). Belfast, Northern Ireland, 2007.

[13] Ramon Dalmau and Xavier Prats. "Controlled time of arrival windows for already initiated energy-neutral continuous descent operations". en. In: *Transportation Research Part C: Emerging Technologies* 85 (Dec. 2017), pp. 334–347. ISSN: 0968090X. DOI: 10.1016/j.trc.2017.09.024. URL: https://linkinghub.elsevier.com/retrieve/pii/S0968090X17302723 (visited on 09/18/2025).

[14] EUROCONTROL. *CDA Implementation Guidance Information*. 2008.

[15] EUROCONTROL. *Continuous Climb and Descent Operations*. 2020. URL: https://www.eurocontrol.int/concept/continuous-climb-and-descent-operations#:~:text=For%20CDO%2C%20the%20study%20concluded,top%20of%20the%20fuel%20CDO (visited on 10/09/2025).

[16] Hartmut Fricke, Christian Seiß, and Robert Herrmann. "Fuel and Energy Benchmark Analysis of Continuous Descent Operations". en. In: *Air Traffic Control Quarterly* 23.1 (Jan. 2015), pp. 83–108. ISSN: 1064-3818, 2472-5757. DOI: 10.2514/atcq.23.1.83. URL: https://arc.aiaa.org/doi/10.2514/atcq.23.1.83 (visited on 10/02/2025).

[17] Anouk Hollebeek. "KDC Mainport Schiphol – Centre of Excellence A collaboration with the Aviation Academy, Amsterdam University of Applied Sciences". Bachelor's Thesis. Schiphol, The Netherlands: Amsterdam University of Applied Sciences, June 18, 2019.

[18] M Inaad. "Fuel and Emission Benefits for Continuous Descent Approaches at Schiphol". Master Thesis. Schiphol, The Netherlands: TU Delft, July 8, 2016. 80 pp.

[19] Daiki Iwata, Yuki Nonaka, and Eri Itoh. "Air traffic control method for more fuel efficient arrivals in terminal airspace". en. In: *Journal of Air Transport Management* 128 (Sept. 2025), p. 102799. ISSN: 09696997. DOI: 10.1016/j.jairtraman.2025.102799. URL: https://linkinghub.elsevier.com/retrieve/pii/S0969699725000626 (visited on 09/11/2025).

[20] J. Ellerbroek J.Hoekstra. *AE4321-15 Air Traffic Management: Lecture Slides*. URL: https://www.eurocontrol.int/sites/default/files/2019-06/lssip2018_netherlands_release.pdf (visited on 10/23/2025).

[21] James Jones et al. "Methods of Selecting Forecast Winds for Flight Management Systems to Support Four Dimensional Trajectory-Based Operations". en. In: *16th AIAA Aviation Technology, Integration, and Operations Conference*. Washington, D.C.: American Institute of Aeronautics and Astronautics, June 2016. ISBN: 978-1-62410-440-4. DOI: 10.2514/6.2016-4069. URL: https://arc.aiaa.org/doi/10.2514/6.2016-4069 (visited on 10/20/2025).

[22] Knowledge and Development Centre Schiphol (KDC). *Applications of ADS-C*. 2014.

[23] Ramon Gomez Ledesma and Francisco A. Navarro. "Continuous descent approaches for maximum predictability". en. In: *2007 IEEE/AIAA 26th Digital Avionics Systems Conference*. Dallas, TX, USA: IEEE, Oct. 2007, 3.A.2–1–3.A.2–8. DOI: 10.1109/DASC.2007.4391871. URL: http://ieeexplore.ieee.org/document/4391871/ (visited on 09/16/2025).

[24] Alan Lee et al. "Performance of Trajectory Models with Wind Uncertainty". en. In: *AIAA Modeling and Simulation Technologies Conference*. Chicago, Illinois: American Institute of Aeronautics and Astronautics, Aug. 2009. ISBN: 978-1-62410-161-8. DOI: 10.2514/6.2009-5834. URL: https://arc.aiaa.org/doi/10.2514/6.2009-5834 (visited on 11/18/2025).

[25] LVNL. *Zelfstudie ATM Kennis*. 2018.

[26] Enrique Juan Casado Magaña. "Trajectory Prediction Uncertainty Moddeling for Air Traffic Management". PhD thesis. University of Glasgow, 2016.

[27] Bjorn Ostertag. *Case study: Using a modern wind uplink*. 2018. URL: https://www.aircraftit.com/articles/using-a-modern-wind-uplink/ (visited on 10/21/2025).

[28] Priyank Pradeep and Peng Wei. "Predictability, variability and operational feasibility aspect of CDA". en. In: *2017 IEEE Aerospace Conference*. Big Sky, MT, USA: IEEE, Mar. 2017, pp. 1–14. ISBN: 978-1-5090-1613-6. DOI: 10.1109/AERO.2017.7943728. URL: http://ieeexplore.ieee.org/document/7943728/ (visited on 09/15/2025).

[29] Mithun Raghunandan. "Evaluating the impact of prediction accuracy on Continuous Descent Operations: The added value of Trajectory Predictor performance through Air-Ground Datalink". Master Thesis. Schiphol, The Netherlands: TU Delft, Feb. 26, 2024. 45 pp.

[30] Falk Sachs et al. "Trials for quiet and efficient flights in advanced continuous descent approach using the low-noise augmentation system LNAS". en. In: *CEAS Aeronautical Journal* 16.2 (Apr. 2025), pp. 613–628. ISSN: 1869-5582, 1869-5590. DOI: 10.1007/s13272-025-00825-2. URL: https://link.springer.com/10.1007/s13272-025-00825-2 (visited on 10/08/2025).

[31] AMS Schiphol. *Facts About Amsterdam Airport Schiphol*. URL: https://www.schiphol.nl/en/aviation-partnerships/amsterdam-airport-schiphol-airport-facts/ (visited on 10/23/2025).

[32] AMS Schiphol. *Flying More Efficient*. URL: https://www.schiphol.nl/en/sustainability/in-the-air/flying-more-efficiently-at-schiphol/?_gl=1*224el5*_up*MQ..*_ga*MzAzMTc5OTg3LjE3NjEzMzE3MDA.*_ga_SY55X9B9Q6*czE3NjEzMzE2OTkkbzEkZzEkdDE3NjEzMzE3MTAkajQ5JGwwJGg1NjY2MjczMjk. (visited on 10/24/2025).

[33] SESAR. *SESAR partners trial solution to make air traffic near airports smoother and more sustainable*. 2022. URL: https://www.sesarju.eu/news/sesar-partners-trial-solution-make-air-traffic-near-airports-smoother-and-more-sustainable#:~:text=One%20of%20the%20promising%20technologies,hour%20capacity%20reduction (visited on 10/09/2025).

[34] Brussels Airport Skeyes. *Continuous descent operations*. 2025. URL: https://www.batc.be/en/statistics/continuous-descent-operations-cdo?date=1759701600&aggregate=week&binary=true (visited on 10/09/2025).

[35] Richard Sopjes et al. "Continuous Descent Approaches with Variable Flight-Path Angles under Time Constraints". en. In: *AIAA Guidance, Navigation, and Control Conference*. Portland, Oregon: American Institute of Aeronautics and Astronautics, Aug. 2011. ISBN: 978-1-60086-952-5. DOI: 10.2514/6.2011-6219. URL: https://arc.aiaa.org/doi/10.2514/6.2011-6219 (visited on 09/11/2025).

[36] Laurel Stell. "Flight management system execution of idle-thrust descents in operations". en. In: *2011 IEEE/AIAA 30th Digital Avionics Systems Conference*. Seattle, WA, USA: IEEE, Oct. 2011, 1E4–1–1E4–15. DOI: 10.1109/DASC.2011.6095979. URL: http://ieeexplore.ieee.org/document/6095979/ (visited on 10/07/2025).

[37] Laurel Stell. "Flight management system prediction and execution of idle-thrust descents". en. In: *2009 IEEE/AIAA 28th Digital Avionics Systems Conference*. Orlando, FL, USA: IEEE, Oct. 2009, pp. 1.C.4–1–1.C.4–12. DOI: 10.1109/DASC.2009.5347570. URL: http://ieeexplore.ieee.org/document/5347570/ (visited on 10/07/2025).

[38] Michael McPartland Tom G. Reynolds. "Exploring Wind Information Requirements for Four Dimensional Trajectory-Based Operations*". In: 11th USA/Europe Air Traffic Management Research and Development Seminar (ATM2015). MIT, June 24, 2015.

[39] Enis T. Turgut, Oznur Usanmaz, and Marc A. Rosen. "Empirical analysis of the effect of descent flight path angle on primary gaseous emissions of commercial aircraft". en. In: *Environmental Pollution* 236 (May 2018), pp. 226–235. ISSN: 02697491. DOI: 10.1016/j.envpol.2018.01.084. URL: https://linkinghub.elsevier.com/retrieve/pii/S0269749117332785 (visited on 09/11/2025).

[40] F J M Wubben and J J Busink. *Environmental benefits of continuous descent approaches at Schiphol Airport compared with conventional approach procedures*. NLR-TP-2000-275. Amsterdam, The Netherlands: Nationaal Lucht- en Ruimtevaartlaboratorium (NLR) — National Aerospace Laboratory, May 2000, p. 11.

[41] Dabin Xue et al. "Low-carbon benefits of aircraft adopting continuous descent operations". en. In: *Applied Energy* 383 (Apr. 2025), p. 125390. ISSN: 03062619. DOI: 10.1016/j.apenergy.2025.125390. URL: https://linkinghub.elsevier.com/retrieve/pii/S0306261925001205 (visited on 09/11/2025).